UNIVERSITY OF CALIFORNIA, SAN DIEGO

Tyrosine phosphorylation of histone H2A by CK2 regulates transcriptional elongation and DNA damage repair

A dissertation submitted in partial satisfaction of the requirements for the degree

Doctor of Philosophy

in

Biomedical Sciences

by

Harihar Basnet

Committee in charge:

Professor Michael Rosenfeld, Chair
Professor Arshad Desai
Professor Christopher Glass
Professor Anthony Hunter
Professor Yang Xu

2014

The Dissertation of Harihar Basnet is approved, and it is acceptable in quality and form for publication on microfilm and electronically:

_____

_____

_____

_____

_____

Chair

University of California, San Diego

2014

TABLE OF CONTENTS

LIST OF FIGURES

ACKNOWLEDGEMENTS

I would like to thank my thesis advisor, Professor Michael G. Rosenfeld, for his guidance and support over the past years. His supervision that involved a balance between independence and guidance taught me to understand and dissect the scientific problems from the core. I would also like to thank the members of my thesis committee, Professor Tony Hunter, Professor Arshad Desai, Professor Christopher K. Glass, Professor Yang Xu and Professor Jean Y. Wang for their advice, time and tremendous support. Professor Hunter's guidance was instrumental for the kinase studies performed in this study.

I would also like to acknowledge present and past members of Rosenfeld laboratory for their valuable insights and thoughtful discussions. I would like to thank Professor Lorraine Pillus for her support and guidance in doing the yeast experiments. I would like to thank Xue B. Su for helping me with the yeast experiments, Dr. Yuliang Tan for doing the bioinformatics analysis of the ChIP-seq experiments, Daria Merkurjev for the alignment of the ChIP-seq experiments, Kenneth A. Ohgi for preparing the library for high throughput sequencing, Jill Meisenhelder for helping with the phosphoamino acid analysis experiments, Dr. Majid Ghassemian (UCSD Mass Spectrometry Core Facility) for helping with mass spectrometric analysis. I would like to thank Professor Karen Arndt (University of Pittsburg) for kindly sharing the *UBP8* null yeast strains.

Chapters 1-4 and 5-9, in part, have been accepted for publication of the material as it may appear in *Nature* 2014. Basnet, Harihar; Su, Xue B.; Tan,

Yuliang; Meisenhelder, Jill; Merkurjev, Daria; Ohgi, Kenneth A.; Hunter, Tony; Pillus, Lorraine & Rosenfeld, Michael G. Nature Publishing Group. 2014. The dissertation author was the primary investigator and author of this paper.

Appendix, in most part, is a reprint of the material that has been accepted for publication as it may appear in *Nature* 2014. Basnet, Harihar; Su, Xue B.; Tan, Yuliang; Meisenhelder, Jill; Merkurjev, Daria; Ohgi, Kenneth A.; Hunter, Tony; Pillus, Lorraine & Rosenfeld, Michael G. Nature Publishing Group. 2014. The dissertation author was the primary investigator and author of this paper.

VITA

EDUCATION

2008-2014	**University of California, San Diego** Ph.D. in Biomedical Sciences	La Jolla, CA
2004-2008	**Hanover College** B.A. Physics and B.A. Mathematics	Hanover, IN

PUBLICATIONS

• **Basnet, H.**, Su, X.B., Tan, Y., Meisenhelder, J., Merkurjev, D., Ohgi, K.A., Hunter, T., Pillus, L. & Rosenfeld, M.G. Tyrosine phosphorylation of histone H2A by CK2 regulates transcriptional elongation. ***Nature***. (Accepted)

• Singh, N.*, **Basnet, H.***, Wiltshire, T., Mohammad, D.H., Thompson, J.R., Heroux, A., Botuyan, M.V., Yaffe, M.B., Couch, F.J., Rosenfeld, M.G.& Mer, G. Dual recognition of phosphoserine and phosphotyrosine in histone variant H2A.X by DNA damage response protein MCPH1. ***PNAS***. 109 (36): 14381-14386 (2012). (* co-first authors)

• Tumaneng, K.**,** Schlegelmilch, K., Russell, R., Yimlamai, D., **Basnet, H.**, Mahadevan, N., Fitamant, J., Bardeesy, N., Camargo, F.D. & Guan, K.L. YAP mediates crosstalk between the Hippo and PI3K-TOR pathways by suppressing PTEN via miR-29. ***Nat Cell Biol***. 14:1322-1329 (2012)

• Veldkamp, C.T., Ziarek, J.J., Su, J., **Basnet, H.**, Lennertz, R., Weiner J.J., Peterson, F.C. & Volkman, B.F. Monomeric structure of the cardioprotective chemokine SDF-1/CXCL12. ***Protein Sci***. 18 (7): 1359-69. (2009).

• Veldkamp, C.T., Seibert, C., Peterson, F.C., Cruz, N.B., Haugner, J.C., **Basnet, H.**, Sakmar, T.P. & Volkman, B.F. Structural Basis of CXCR4 Sulfotyrosine Recognition by the Chemokine SDF-1/CXCL12. ***Sci Signal***. 1 (37). (2008).

• **Basnet, H.** Design of a Chemical Engine. ***Nepal Journal of Science and Technology***. 4: 67-70. (2002)

ABSTRACT OF THE DISSERTATION

Tyrosine phosphorylation of histone H2A by CK2 regulates transcriptional elongation and DNA damage repair

by

Harihar Basnet

Doctor of Philosophy in Biomedical Sciences

University of California, San Diego, 2014

Professor Michael Rosenfeld, Chair

In eukaryotes, genomic DNA is packaged into histone proteins, which can undergo post-translational modifications that are in turn critical in regulating transcription, the cell cycle, DNA replication, and DNA damage repair. In this study, we identify a novel tyrosine phosphorylation in histone H2A (Y57) that is conserved from yeast to mammals. Surprisingly, the phosphorylation is mediated by an unsuspected tyrosine kinase activity of casein kinase 2 (CK2). Mutation of the Y57 residue or inhibition of CK2 activity impairs transcriptional elongation, marked by a decrease in the recruitment of RNA polymerase II

across active genes in yeast as well as mammalian cells. Genome-wide binding analysis reveals that CK2 alpha, the catalytic subunit of CK2, binds across RNA polymerase II-transcribed coding genes and active enhancers. Mutation of Y57 causes a defect in transcriptional elongation and DNA damage repair. At the molecular level, Y57 mutation causes a dramatic loss of H2B mono-ubiquitylation as well as H3K4me3 and H3K79me3 (histone marks associated with active transcription), a decrease in H2A mono-ubiquitylation and an increase in H2A S128 (H2AX S139 in mammals) phosphorylation (histone mark associated with DNA damage). Mechanistically, both CK2 inhibition and H2A-Y57F mutation antagonize the H2B deubiquitylation activity of the SAGA complex, suggesting a critical role of this novel phosphorylation event in coordinating the activity of the SAGA complex during transcription and DNA damage repair. Together, these results identify a new component of regulation in transcriptional elongation and DNA damage repair based on CK2-dependent tyrosine phosphorylation of the globular domain of H2A.

Introduction

The major achievement of the last century in life sciences is the leap in our understanding about the details of life at the molecular level. It is now clear that the blueprint of life resides in the deoxyribonucleic acid (DNA) that is compacted into the nucleus. The DNA sequence called genome provides an identity not only to a species but also to an individual within a species. The specific sequences responsible for this defining role remain to be identified. Although there is a difference in the DNA sequence between species and individuals, the majority of machineries within the cells are conserved from a simple one-celled organism like yeast to a complex organism like human. Regardless of the origin, each eukaryotic cell uses common fundamental machineries that maintain genomic integrity and regulate the expression of genes that are present in the genome. An integral part of the genome are proteins called histones, which are highly conserved both in sequence and structure among species, and are important in packaging the long genome within a small nucleus. Since genomic DNA is directly associated with histones, these proteins play a central role in determining the accessibility of the genome which in turn is critical in modulating gene expression and maintaining genomic integrity.

Histones and their post-translational modifications

Histones are highly basic proteins between 11-40 KDa in size. There are five different histones namely H2A, H2B, H3, H4 and H1. Two of each H2A, H2B, H3 and H4 form an octamer, which is encompassed by one and a half turns

of genomic DNA (146 base pairs) to form a fundamental structure of chromatin called nucleosome[1] (**Fig. 1)**. Two nucleosomes are connected together by the linker histone H1. The structural and functional diversity in nucleosomes are achieved primarily through the presence of different variants of histones and their post-translational modifications.

Each histone has several variants with some minor difference in the amino acid sequence[2–8], and these differences play an important role in establishing functional diversity in the nucleosomes. For example, H2AX is an H2A variant that has some additional amino acids on the C-terminus tail, which confer an additional role in DNA damage repair (DDR)[9–11]. Likewise, H3.3, an H3 variant, has a few amino acid differences, and is specialized in gene activation[2,4,7]. Although different histone variants play important roles in regulating different biological functions such as regulation of gene expression, cell cycle and DDR, extensive post-translational modifications in histones play key roles in regulating different biological processes[12,13]. Post-translational modifications in histones include phosphorylation, methylation, acetylation, ubiquitylation, adenosine diphosphate ribosylation, sumoylation, and citrullination[12,14] **(Fig. 1)**. These modifications can affect chromatin compaction directly by virtue of the change in net charge in histones caused by such post-translational modifications. For instance, phosphorylation adds negative charge to histones, and acetylation neutralizes the positive charge of the lysine residue. In many cases, post-translational modifications often modulate the binding of other chromatin

remodeling/modifying proteins, which can in turn alter chromatin structure. Many chromatin-remodeling/modifying proteins have highly conserved domains that interact specifically with modified proteins[15–18]. For example, BRCA1 C-terminus (BRCT) domain binds to phospho-serine[19,20], Forkhead associated (FHA) domain to phospho-threonine[21], Plant Homeo Domain (PHD), Tudor domain and PWWP (Pro-Trp-Trp-Pro) domain to methylated proteins[15,18,22], Bromo domain to acetylated proteins[16], and Src homology 2 (SH2) domain to phospho-tyrosine[23]. In some cases, post-translational modifications in histones can modulate the function of other enzymes allosterically[24–26]. Thus, post-translational modifications in histones can directly affect chromatin compaction or indirectly regulate compaction by modulating the recruitment/activity of other proteins involved in chromatin modification or remodeling.

With the advancement in Mass Spectrometry (MS), a large number of histone modifications have been identified[6,14,27], though the list may still be far from complete. Even among the identified histone modifications, only a few of them have been well characterized. In many cases, the mechanisms that regulate the functionally characterized modifications are poorly understood.

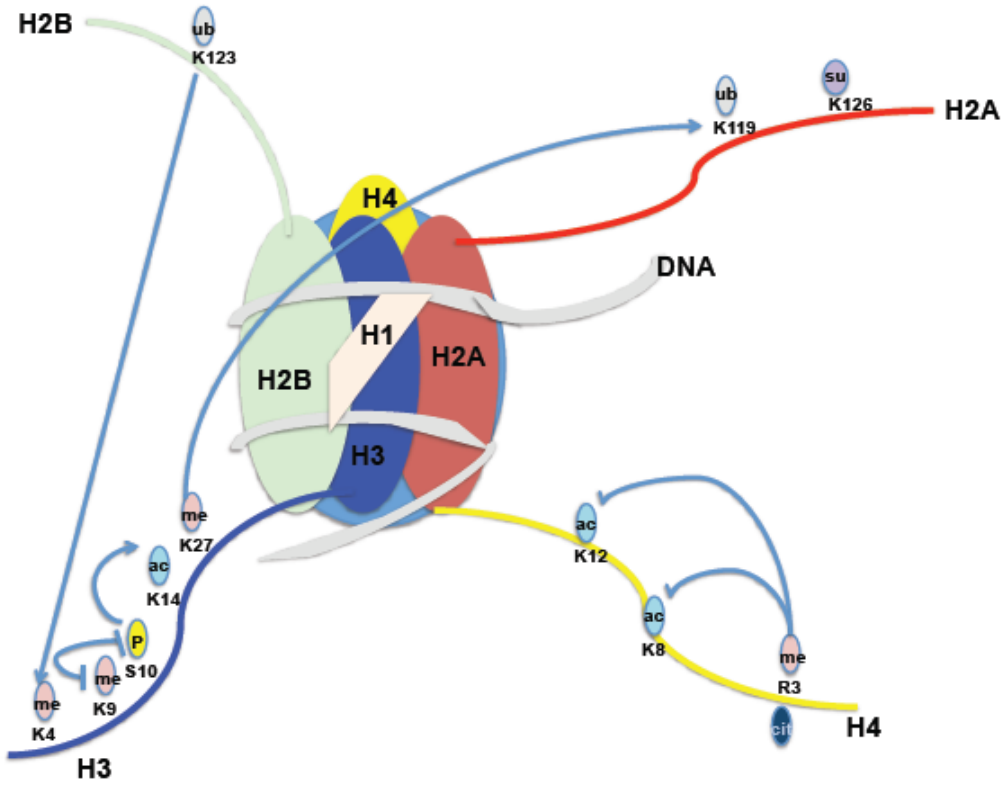

Figure 1. Diagram of a nucleosome. Structure of a nucleosome showing the histones (H2A, H2B, H3, H4 and H1), DNA and some post-translational modifications of the histone tails along with few characterized crosstalks between histone modifications.

Histone ubiquitylation

One of the most abundant post-translational modifications in histones is the addition of a small 8.5-kDa protein called ubiquitin to the lysine residue (K) through a process called ubiquitylation[28]. Ubiquitylation occurs through the coordinated action of three different enzymes[29], namely, E1-ubiquitin activating enzyme (E1), E2-ubiquitin conjugating enzyme (E2) and E3-ubiquitin ligase (E3). The E3 ligases can add a single ubiquitin or a chain of poly-ubiquitin during the reaction. In the case of poly-ubiquitylation, the chains are commonly linked

through K48 or K63 residue in the ubiquitin. K48-linked polyubiquitylation usually targets proteins for degradation through proteasomes[30] whereas K63-linked polyubiquitylation acts as a signaling modification[31]. Ubiquitylation is a dynamic process, and this modification can be removed by another class of enzymes called deubiquitylases (DUBs)[32].

All five histones have been reported to be ubiquitylated[28,33–36]. The majority of ubiquitylation exist as mono-ubiquitylation, which regulates chromatin structure rather than targeting the protein for degradation[28,37]. H3, H4, and H1 ubiquitylation is less abundant compared to H2A and H2B ubiquitylation, and the actual functions of these modifications are yet to be characterized. On the other hand, H2A and H2B ubiquitylation is very abundant, and their functional significance has been well studied[37–48]; it is estimated that H2A mono-ubiquitylation accounts for about 5-15% of total H2A, and H2B mono-ubiquitylation is about 1-2% in vertebrates[33].

H2B mono-ubiquitylation is highly conserved from yeast to mammals (Lys 123 in yeast and Lys 120 in mammals), and is primarily involved in transcriptional elongation[45,49]. Most of the functional studies on H2B mono-ubiquitylation have been carried out in the yeast system. In yeast, ubiquitylation is mediated by the Rad6/Bre1 ubiquitin ligases[50,51], and has been shown to be necessary for the establishment of other important histone marks like H3K4 and H3K79 methylations[52]. Furthermore, components of the polymerase II associated factor (Paf1) complex, such as Paf1 and Rtf1, have also been shown to be essential for

the establishment of H2B mono-ubiquitylation[51,53,54]. Two DUBs, Ubp10 and Ubp8, have been shown to deubiquitylate H2B in yeast[55–57]. Ubp8 is the major H2B DUB that is a component of the Spt-Ada-Gcn5 Acetyl transferase (SAGA) complex and has been shown to play an important role in transcriptional elongation[55]. Normally, the addition and removal of a post-translational modification serve opposite functions; however in the case of H2B mono-ubiquitylation, both ubiquitylation and deubiquitylation positively regulate transcriptional elongation[55]. Another mystery associated with this post-translational modification is that the ubiquitylation machinery and the deubiquitylase complex are both localized in actively transcribed regions[53–55], though the mechanism that coordinates the activity of the two complexes remains unknown[58]. The Ubp10 deubiquitylase, on the other hand, is involved in telomerase silencing[56,57].

H2A mono-ubiquitylation is also a highly conserved post-translational modification that exists abundantly in multi-cellular organisms; however it is undetectable in the budding yeast[28,58]. Unlike H2B mono-ubiquitylation, H2A mono-ubiquitylation is more complex in terms of the number of sites that are ubiquitylated, the enzymes involved, and the associated functions. H2B ubiquitylation occurs primarily on one site (K123 in yeast and K120 in mammals); however, H2A has been shown to ubiquitylated at multiple sites (K13, K15, K118 and K119)[47,59]. Ring1/Ring2 (enzymatic components of the Polycomb Repressor Complex (PRC) 1), 2A-HUB, RNF8, BRCA1, and RNF168 have been shown to

ubiquitylate H2A[39,46,47,59–62], while USP16, USP21, 2A-DUB, and BAP1 have been shown to deubiquitylate H2A[38,40,43,63]. It is noteworthy that both H2A and H2B can be deubiquitylated by the SAGA complex[64], which is the only common link between H2A and H2B mono-ubiquitylation identified so far. This modification has been shown to play diverse functions, that include gene silencing, X-chromosome inactivation, cell cycle regulation, DDR, and transcriptional activation[38–41,43,46,47,59,60,62,63,65,66] **(Fig. 2)**.

Despite the broad roles of H2A and H2B deubiquitylation, very little is known about the molecular mechanism that regulates such modification under different biological contexts. In 2002-2003, it was reported that the PHD domain of the CBX subunit of the PRC1 complex interacts with H3K27me3 that is created by the PRC2 complex, targeting the PRC1 complex to specific loci to regulate H2A mono-ubiquitylation[67–69]. This result was further supported by the co-localization of PRC1 and PRC2 in chromatin[70]. However, in the following years, it became clear that the PRC2 complex is not required for the creation of H2A mono-ubiquitylation[65,71,72]. These findings indicate that there are additional mechanisms that are involved in the regulation of H2A mono-ubiquitylation.

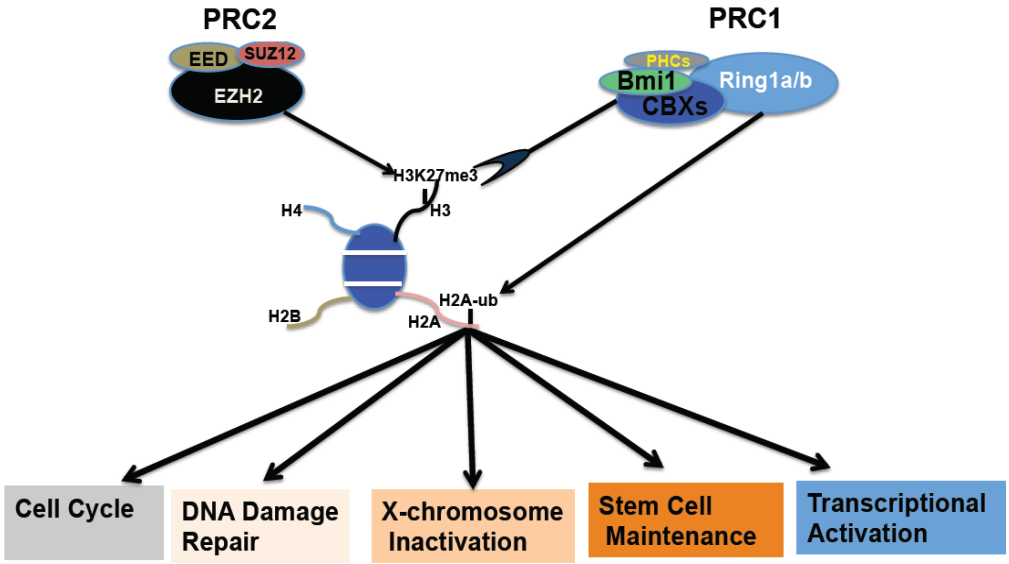

Figure 2. Diagram showing regulation and roles of H2A mono-ubiquitylation. A diagram representation of current understanding about the regulation and roles of H2A mono-ubiquitylation in different biological processes.

Crosstalk between histone modifications

One common mode of regulation of histone modifications is crosstalk between modifications **(Fig. 1)**. Basically, one post-translational modification in a histone can affect another modification by recruiting the writer or the eraser of the other modification, or by enhancing or inhibiting the activity of another enzyme allosterically[43,73,74]. For instance, H2B mono-ubiquitylation regulates H3K4 methylation by regulating the binding of the Cps35 subunit of the COMPASS complex that creates H3K4 methylation[44]. Likewise, deacetylation of the H3 N-terminal tail facilitates H3S10 phosphorylation by Aurora kinase[75]. Numerous examples of such crosstalks among histone modifications have been described[44,73,76]. The existence of a potential crosstalk between H2A mono-ubiquitylation and other histone modifications remains largely unexplored. In

non-histone proteins, there are several examples of crosstalks between ubiquitylation and phosphorylation[76], suggesting the possibility that a crosstalk between phosphorylation and ubiquitylation in H2A might exist. Indeed, testing this hypothesis revealed a novel phosphorylation in the Y57 residue in H2A that is found to regulate H2A mono-ubiquitylation in the K119 residue in H2A as well as H2B mono-ubiquitylation in yeast. Casein kinase 2 (CK2) is identified as the kinase responsible for this phosphorylation, which is shown to occur in the context of the nucleosome rather than the full-length soluble protein. Y57 phosphorylation is also found to be an important regulator of H3K4me3, H3K79me3, and H2A-S128 phosphorylation in yeast. Mechanistically, Y57 phosphorylation is shown to antagonize the DUB activity of the SAGA complex. Furthermore, Y57 is shown to be important for cell-growth, transcriptional elongation, and DDR. Last but not least, a novel function of CK2 in regulating transcriptional elongation in yeast as well as mammalian cells is uncovered.

Chapter 1. A novel H2A-Y57 phosphorylation regulates H2A-ubiquitylation *in cis*

To test the hypothesis that a crosstalk exists between phosphorylation and ubiquitylation in H2A, we generated a mutant library of Flag-tagged H2AX, a common variant of H2A, in which we mutated each serine/threonine residue to alanine and each tyrosine residue to phenylalnine, and tested the effects of these mutations on ubiquitylation. H2AX was used in this study as it includes a few additional serine/threonine/tyrosine residues along with all the ones present in canonical H2A, thus allowing us to detect any crosstalk that is present only in H2AX as well. The H2AX mutants were expressed in 293T cells, and the level of mono-ubiquitylation in each mutant was measured by immunoblotting. Mono-ubiquitylated H2AX migrates more slowly in the gel, and could be detected as a shifted band in immunoblotting experiments. Thus, the antibody against the Flag tag or H2AX could be used to determine the level of total H2AX and mono-ubiquitylated H2AX. Previous studies have verified that the shifted band is mono-ubiquitylated H2AX, not other ubiquitin-like modifications[59]. We measured the level of H2AX mono-ubiquitylation by Flag antibody, and found that mutation of the Y57 residue resulted in a reduced level of mono-ubiquitylation **(Fig. 3a)**. Since the Y57 residue is conserved in canonical H2A, we tested if similar regulation occurs in canonical H2A as well. Indeed, Y57 mutation resulted in a decreased level of H2A mono-ubiquitylation **(Fig. 3b)**. Next, to eliminate the possibility that the observed regulation is an artifact of transient over-expression,

we made stable 293T cells expressing either WT or Y57F mutant H2A/H2AX, and measured the level of mono-ubiquitylation by immunoblotting. This experiment also showed a decrease in the level of mono-ubiquitylation in the Y57F mutant **(Fig. 3c)**, suggesting that phosphorylation in the Y57F residue in H2A/H2AX might potentially regulate mono-ubiquitylation in H2A/H2AX. H2A is ubiquitylated in several residues (K119, K118, K13 and K15). We therefore tested whether mutation in Y57 specifically affects ubiquitylation in a specific residue. Since only the antibody specific for K119-ubiquityl H2A is available, we first tested if Y57F mutation affects ubiquitylation in the K119 residue. We immunoprecipitated WT and H2A-Y57F mutant under denaturing conditions and immunoblotted with the H2A-K119 ubiquityl antibody. Interestingly, we found that K119 ubiquitylation was defective in the H2A-Y57F mutant **(Fig. 3d)**. The immunoprecipitation was carried out under denaturing conditions to eliminate background from interacting proteins. The lysine mutants of H2A demonstrated the specificity of the antibody **(Fig. 3d)**. The Y57 residue in H2A is located in the globular region of H2A, which suggests the possibility that mutation of this residue causes some structural defects that lead to the observed reduction in H2A mono-ubiquitylation. To address this, we examined whether Y57 mutation in H2A makes the protein non-functional. To do this, we used an elegant genetic system that can test if the mutation makes H2AX non-functional *in vivo*. Functional H2AX is required for the formation of DNA damage induced MDC1 and 53BP1 foci formation[77,78]. Thus, we reconstituted *H2AX-/-* MEFs with either WT or H2AX-Y57F, and tested if the mutant H2AX can rescue the defect of DNA

damage-dependent MDC1 and 53BP1 foci formation. The reconstituted MEFs were treated with gamma irradiation to induce DNA damage. Like WT H2AX-reconstituted MEFs, H2AX-Y57F-reconstituted MEFs formed DNA damage-dependent MDC1 and 53BP1 foci **(Fig. 3e)**, demonstrating that Y57F mutation in H2AX does not compromise the functionality of the protein. Next, we tested if the residue is phosphorylated. Flag-tagged tyrosine mutants of H2A were expressed in 293T cells, immunoprecipitated under denaturing conditions, and immunoblotted with pan phospho-tyrosine antibody. This experiment showed a decreased level of phosphorylation in Y39F and Y57F mutants suggesting that these residues might be phosphorylated **(Fig. 3f)**. Finally, we employed Mass Spectrometry (MS) to verify the physical existence of H2A-Y57 phosphorylation *in vivo*. Histone extracts from 293T cells were digested with trypsin, and post-translational modifications in the proteins were analyzed by MS. As expected, we observed several peptides with H2A-Y57 phosphorylation **(Fig. 3g)**, firmly establishing the existence of H2A-Y57 phosphorylation *in vivo*.

Chapter 1, in part, has been accepted for publication of the material as it may appear in *Nature* 2014. Basnet, Harihar; Su, Xue B.; Tan, Yuliang; Meisenhelder, Jill; Merkurjev, Daria; Ohgi, Kenneth A.; Hunter, Tony; Pillus, Lorraine & Rosenfeld, Michael G. Nature Publishing Group. 2014. The dissertation author was the primary investigator and author of this paper.

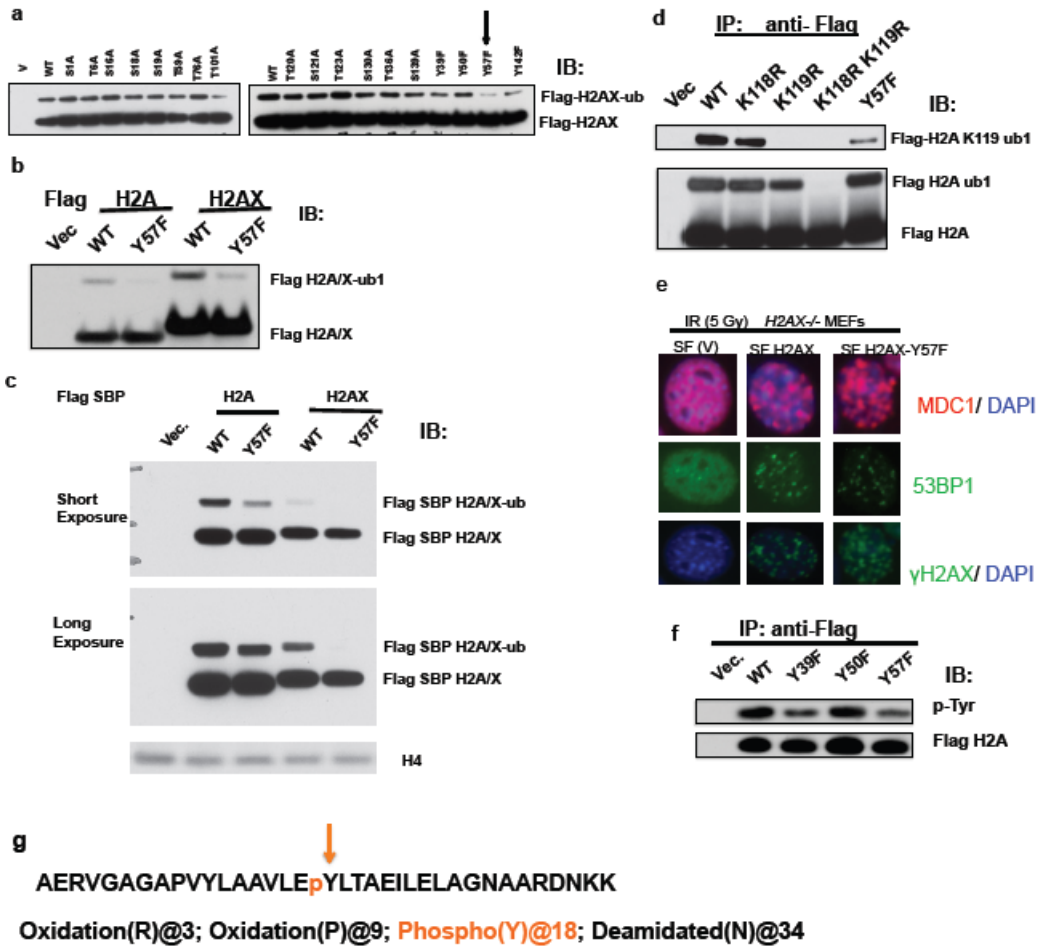

Figure 3. **A novel H2A-Y57 phosphorylation regulates H2A-ubiquitylation *in cis.*** **(a-d)** Mutation in Y57 in H2A/H2AX affects mono-ubiquitylation *in cis*. **(a)** Serine/threonine and tyrosine residues in Flag-H2AX were mutated to alanine and phenylalanine respectively, expressed in 293T cells, and monou-biquitylation in the mutant H2AX was evaluated by immnoblotting using Flag antibody. Arrow indicates the Y57 residue. **(b)** Flag- H2A/H2AX or Y57F mutant was transiently expressed in 293T cells, and the level of mono-ubiquitylation was measured by immunoblotting using Flag antibody. **(c)** Flag-SBP WT or Y57F mutant H2A/ H2AX was stably expressed in 293T cells, and the level of H2A/ H2AX mono-ubiquitylation was measured by immunoblotting using Flag antibody. **(d)** Indicated H2A mutants were expressed in 293T cells, immunoprecipitated under denaturing conditions, and immunoblotted with indicated antibodies. **(e)** H2A-Y57F mutant protein is functional. *H2AX-/-* MEFs were reconstituted with either Vector (SF), SF-WT H2AX or SF-H2AX-Y57F, and immunostained for the indicated antibodies after irradiation. **(f, g)** The Y57 residue in H2A is phosphorylated. **(f)** Indicated Flag-tagged H2A mutants were expressed in 293T cells, immunoprecipitated under denaturing conditions, and immunoblotted with the indicated antibodies. **(g)** Histone extracts from 293T cells were digested with trypsin, and post-translational modifications in histones were analyzed by Liquid Chromatography (LC)-MS. Shown is an H2A peptide with phosphorylation in the Y57 residue. Arrow indicates the Y57 residue.

Chapter 2. Testing of H2A-Y57 phospho antibody

To further characterize the function of H2A-Y57 phosphorylation, we developed an antibody specific for phosphorylated H2A-Y57. The specificity of the antibody was tested by peptide blocking assay, calf intestinal phosphatase (CIP) treatment, and dot blot assay. The antibody detected proteins corresponding to the size of H2A, H2A-ub1, and H2A-ub2 **(Fig. 4a)**, and the antibody signal was blocked when it was pre-incubated with H2A peptide phosphorylated at Y57 but not with the corresponding unphosphorylated H2A peptide **(Fig. 4a)**. The dot blot assay also showed specific recognition of the phosphorylated peptide **(Fig. 4b)**. Likewise, histone extracts dephosphorylated by CIP treatment showed a reduced signal compared to mock-treated samples **(Fig. 4c)**. Collectively, these results demonstrate the phospho-specificity of the antibody.

Chapter 2, in part, has been accepted for publication of the material as it may appear in *Nature* 2014. Basnet, Harihar; Su, Xue B.; Tan, Yuliang; Meisenhelder, Jill; Merkurjev, Daria; Ohgi, Kenneth A.; Hunter, Tony; Pillus, Lorraine & Rosenfeld, Michael G. Nature Publishing Group. 2014. The dissertation author was the primary investigator and author of this paper.

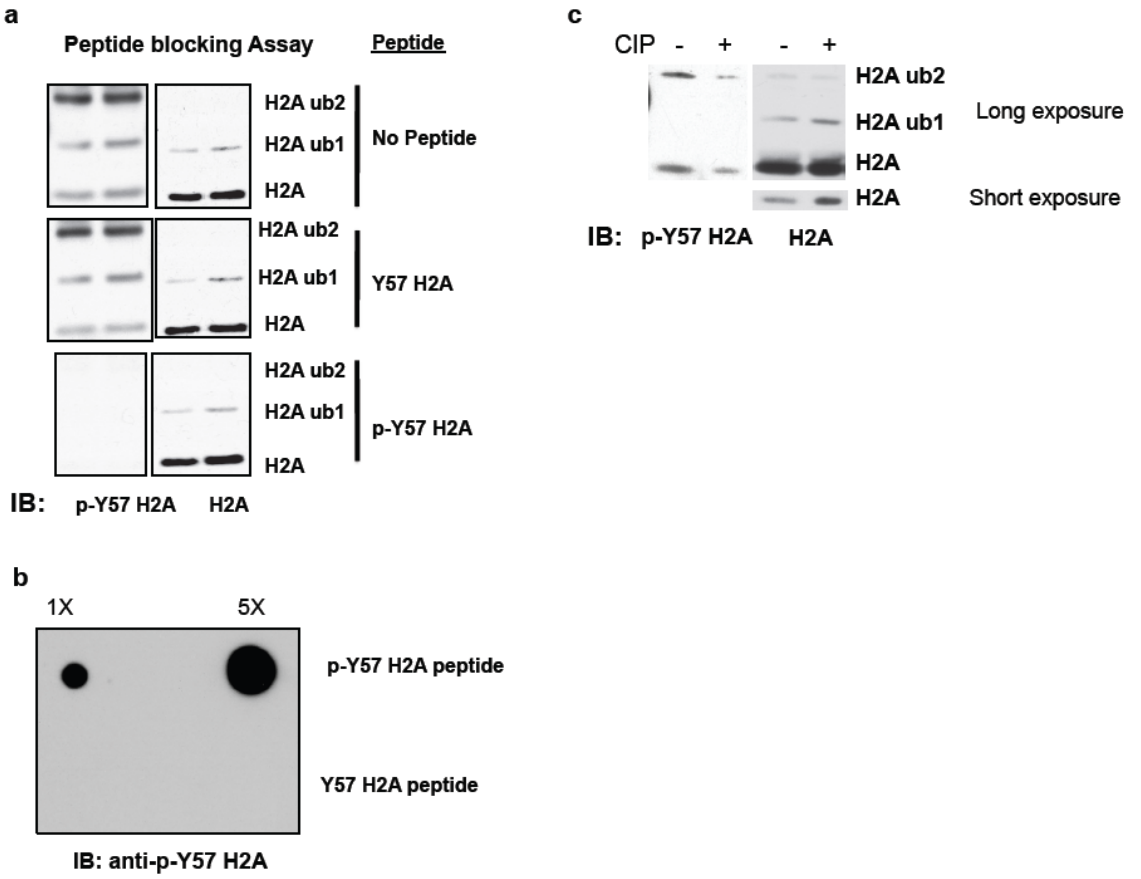

Figure 4. Testing of H2A-Y57 phospho antibody. (a-c) H2A-Y57 phospho antibody specifically detects phospho-H2A. **(a)** Nuclear extracts from 293T cells were immunoblotted with anti-p-Y57 H2A pre-incubated with indicated peptides, and re-probed with anti-H2A. **(b)** The anti-phospho-Y57-H2A antibody specifically recognizes H2A peptide phosphorylated at Y57 but not the unphosphorylated peptide. Indicated peptides were spotted on nitrocellulose, and probed with anti-phospho-Y57 H2A. **(c)** Histone extracts from 293T cells were treated with calf intestinal phosphatase (CIP) for 1 hour, and immunoblotted as indicated.

Chapter 3. H2A-Y57 is phosphorylated in yeast, and is required for normal growth.

We next investigated the biological role of H2A-Y57 phosphorylation. The most rigorous approach to identify the biology associated with a post-translational modification in a protein would be to mutate the residue, and dissect the phenotype caused by the mutation. In mammals, there are multiple genomic copies of H2A, and the Y57 residue is conserved in all variants of H2A **(Fig. 5a)**. Thus, it would be technically challenging to perform mutational studies in the mammalian system. Hence, we considered budding yeast to test the function of this novel phosphorylation, as it contains only three H2A variants, and point mutational study in histones is possible[79,80]. The fact that the Y57 residue is highly conserved from yeast to mammals **(Fig. 5b)** and that most of the important histone modifications are also conserved from yeast to mammals[12,15,44,50,81,82] make budding yeast a viable system to study the function of H2A-Y57 phosphorylation. However, previous studies have shown that mutation of Y57 to alanine causes lethality in yeast[79,80]. Structurally, alanine lacks the aromatic ring of tyrosine along with the hydroxyl group **(Fig. 5c)**. It is possible that the aromatic ring in the globular domain of H2A has a critical structural role. We therefore made a more conservative substitution for tyrosine with phenylalanine that contains the aromatic ring but only misses the hydroxyl group that can be phosphorylated **(Fig. 5c)**, and tested if the Y-to-F mutation exhibits a different phenotype. To our great surprise, we found that H2A-Y58F mutant yeast was

viable, and showed a slow growth phenotype **(Fig. 5d)**. Y57 in mammals corresponds to the Y58 residue in budding yeast **(Fig. 5b)**. However, the same mutation caused lethality in *HTZ1* (a variant of H2A encoding H2AZ)-null background **(Fig. 5d)**. H2AZ plays a role in transcriptional activation[83–86], and *HTZ1* deletion alone shows a mild defect in growth **(Fig. 5d)**. This result demonstrates that there is a negative genetic interaction between H2AZ and H2A-Y58F mutation, and suggests an important role of H2A-Y58 phosphorylation in transcriptional activation. In H2AZ, the residue corresponding to Y57 (Y65) and surrounding amino acids are conserved. We next investigated the effect of double mutation of the corresponding tyrosine residues in both H2A and H2AZ on growth. We found that the double mutation caused an extremely slow growth phenotype but rescued the lethality in *HTZ1* deletion **(Fig. 5e)**. This result indicates that the potential H2A-Y58 phosphorylation is not essential for survival. Next, we tested if the residue is phosphorylated in yeast. Flag-tagged WT and H2A-Y58F were expressed along with untagged WT H2A as a control in yeast, and whole cell extracts (WCEs) were immunoprecipitated under denaturing conditions using Flag antibody, and tyrosine phosphorylation was measured by pan-phospho-tyrosine antibody. The level of tyrosine phosphorylation was reduced in H2A-Y58F yeast compared to the WT **(Fig. 5f)**, indicating that this residue is possibly phosphorylated. As expected, phosphorylation was also detected by an antibody specific to phospho-H2A-Y57 when WCEs from WT and H2A-Y58F yeast were immunoblotted **(Fig. 5g)**.

Chapter 3, in part, has been accepted for publication of the material as it may appear in *Nature* 2014. Basnet, Harihar; Su, Xue B.; Tan, Yuliang; Meisenhelder, Jill; Merkurjev, Daria; Ohgi, Kenneth A.; Hunter, Tony; Pillus, Lorraine & Rosenfeld, Michael G. Nature Publishing Group. 2014. The dissertation author was the primary investigator and author of this paper.

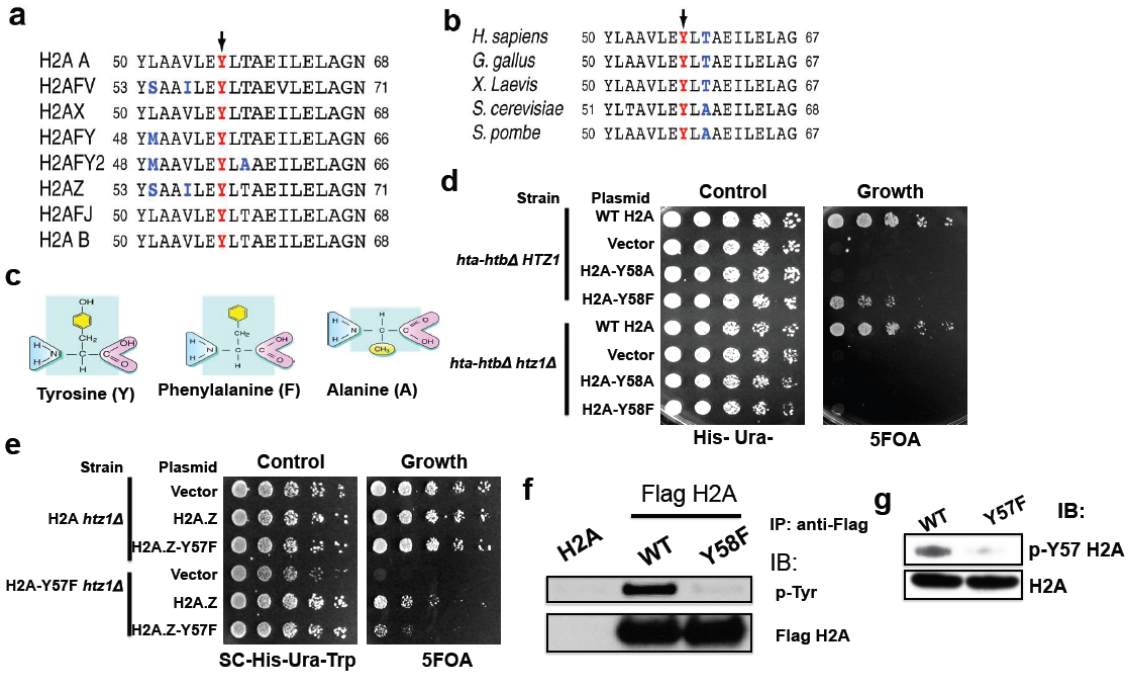

Figure 5. H2A-Y57 is phosphorylated in yeast, and is required for normal growth. **(a)** The Y57 residue is conserved in all variants of H2A. Sequence of indicated H2A variants in mammals surrounding the Y57 residue (arrow) is shown. **(b)** The Y57 residue in H2A is highly conserved. Comparison of H2A sequence surrounding the Y57 residue (arrow) in the indicated organisms is shown. **(c)** Structure of tyrosine, alanine, and phenylalanine is shown. **(d)** The conserved Y58 residue in H2A is required for normal growth, and H2A-Y58F mutation is lethal in the absence of H2AZ in yeast. Five-fold serial dilutions of the following transformants were plated on SC-His-Ura for growth control and 5-FOA for the removal of pJH33: *hta-htbΔ HTZ1* (LPY14461) and *hta-htbΔ htz1Δ* (LPY19236) strains were transformed with WT H2A (pLP2133), pRS313 (vector), H2A-Y58A (pLP3211) or H2A-Y58F (pLP3213). **(e)** The H2A-Y58 residue has overlapping functions with the H2AZ-Y65 residue in yeast. Five-fold serial dilutions of the following transformants were plated on SC-His-Ura-Trp for growth and 5-FOA for the loss of pJH33: H2A *htz1Δ* (LPY19259) and H2A-Y58F *htz1Δ* (LPY19261) were transformed with pRS314 (vector), H2AZ (pLP2252) or H2AZ-Y65F (pLP3200). **(f, g)** The Y58 residue in H2A is phosphorylated in *S. cerevisiae*. **(f)** Flag-tagged H2A and H2A-Y58F were immunoprecipitated from WT (LPY14828) and H2A-Y58F (LPY19464) cells under denaturing conditions using anti-Flag antibody and immunoblotted with the indicated antibodies. **(g)** Whole cell extracts were prepared under denaturing conditions and immunoblotted as indicated.

Chapter 4. H2A-Y57/58 phosphorylation regulates transcriptional elongation

Next, we investigated the role of H2A-Y58 phosphorylation by dissecting the phenotype of the H2A-Y58F yeast. Distinct post-translational modifications in histones are involved in distinct biological functions. For example, phospho-Ser139-H2AX is specifically involved in DNA damage repair[9–11,20,77,87,88]. Likewise, H2B-ub, H3K36me3, and H3K79me2/3 are involved in transcriptional elongation[45,55,89–91], while H3S10 phosphorylation is involved in mitosis[92,93]. Analysis of histone modifications in H2A-Y58F yeast could provide some information on the biological processes that are affected by the mutation. We examined several histone modifications that are known to be involved in DNA damage repair, cell cycle, and transcription in the H2A-Y58F yeast. Regarding the modifications involved in transcriptional regulation, H2A-Y58F mutation specifically lowered the levels of H2B-ub, H3K4me3, and H3K79me3 **(Fig. 6a)**, while the same mutation caused a moderate increase in H3K27 acetylation **(Fig. 6a)**. This result is of particular significance because H2B-ub has been established to be involved in transcriptional elongation[45,49], and H2B-ub has also been reported to positively regulate H3K4me3 and H3K79me3[52], histone modifications associated with transcriptional elongation, suggesting the likelihood that H2A-Y58F mutation might affect transcriptional elongation. To assess the effect of H2A-Y58F mutation on transcriptional elongation, we tested if the mutant yeast shows growth sensitivity to 6-azauracil (6-AU). 6-AU inhibits IMP

dehydrogenase that is necessary for the synthesis of GTP, and such inhibition lowers the level of endogenous GTP and causes growth defects resulting from impaired transcriptional elongation[53,54]. As anticipated, the H2A-Y58F mutant yeast showed sensitivity to 6-AU, indicating a defect in transcriptional elongation **(Fig. 6b)**.

At the molecular level, transcriptional elongation is defined by the traveling of RNA polymerase II (Pol II) from the promoter to the gene body. We tested if there is a defect in Pol II binding in the gene body of actively transcribed genes in the H2A-Y58F yeast strain by chromatin immunoprecipitation (ChIP) followed by quantitative polymerase chain reaction (qPCR). In yeast, increasing the culture temperature from 30°C to 37°C induces the expression of heat shock genes. In other words, the increase in temperature causes the recruitment of Pol II to the gene bodies of heat shock-induced genes. We then checked if the binding of Pol II in the heat shock-induced genes is compromised in the H2A-Y58F yeast upon heat shock. Consistent with the 6-AU assay result, we found that Pol II binding was reduced in several heat shock-induced genes[94] in yeast carrying the H2A-Y58F mutation **(Fig. 6c)**. The defect was further increased in yeast carrying Y-to-F mutations in both H2A and H2AZ (Y65F) **(Fig. 6c)**. In addition, Pol II binding was reduced in the gene body of *PYK1*, a housekeeping gene **(Fig. 6c)**. To ensure that the observed reduced binding of Pol II was not due to reduced expression of Pol II in the H2A-Y58F yeast, we examined the protein level of Pol II in WT and the H2A-Y58F yeast, and found that the Pol II large subunit protein

level was comparable in WT and the H2A-Y58F yeast **(Fig. 6d)**. Since the output of transcription is messenger ribonucleic acid (mRNA), we tested if the defect in transcriptional elongation is also reflected at the mRNA level. We detected a lower level of mRNA of the corresponding genes in the mutant yeast by reverse transcription (RT)-real time qPCR, further supporting the role of H2A-Y58 phosphorylation in transcriptional elongation **(Fig. 6e)**. We also tested the effect of the mutation in H2AZ alone on transcription by RT-qPCR, and found that there is a mild effect in the heat shock induced genes **(Fig. 6f)**.

While the mutational results in yeast strongly suggested a role for H2A-Y58 phosphorylation in transcriptional elongation, it cannot be ruled out that the observed phenotype is due to the loss of the hydroxyl group of the tyrosine rather than a loss in Y58 phosphorylation itself. To address this, we developed an assay to test if H2A-Y57 phosphorylation is involved in transcriptional elongation. Flavopiridol is a drug that blocks transcriptional elongation by inhibiting the CDK9 mediated kinase activity of Positive transcriptional elongation factor b (PTEF b)[95]. We treated 293T cells with flavopiridol, released the inhibition by washing out the drug, and checked H2A-Y57 phosphorylation. Like H2B mono-ubiquitylation, which marks transcriptional elongation, we found that flavopiridol treatment resulted in a decrease in H2A-Y57 phosphorylation, and the phosphorylation is restored upon removal of the drug **(Fig. 6g)**. A control histone mark, H3K4me2, did not change with the drug treatment **(Fig. 6g)**. A change in p-Ser2 C-terminal domain (CTD) of Pol II, substrate of PTEF b, verified that the assay worked.

Collectively, these results demonstrate a role of H2A-Y57/58 phosphorylation in transcriptional elongation.

Chapter 4, in part, has been accepted for publication of the material as it may appear in *Nature* 2014. Basnet, Harihar; Su, Xue B.; Tan, Yuliang; Meisenhelder, Jill; Merkurjev, Daria; Ohgi, Kenneth A.; Hunter, Tony; Pillus, Lorraine & Rosenfeld, Michael G. Nature Publishing Group. 2014. The dissertation author was the primary investigator and author of this paper.

Figure 6. H2A-Y57/58 phosphorylation regulates transcriptional elongation (a) H2A-Y58F mutation specifically diminishes H2B mono-ubiquitylation, and H3K4- and H3K79-trimethylation marks. Whole cell extracts from WT (LPY17876) and H2A-Y58F (LPY17878) strains were immunoblotted as indicated. Each lane is an independent biological sample. **(b-e)** H2A-Y58F mutant cells are defective in transcriptional elongation. **(b)** Five-fold serial dilutions of WT (LPY18192) and H2A-Y58F (LPY18194) cells were plated on SC supplemented with NH_4OH (solvent) or 100µg/mL 6-azauracil (6-AU). **(c)** Pol II binding was reduced in tyrosine mutants of H2A and H2AZ. Pol II binding in the indicated genes was measured by ChIP-qPCR in WT H2A (LPY17876), H2A-Y58F (LPY19806), and H2A-Y58F H2AZ-Y65F (LPY19894) cells that were grown at 30°C or shifted to 37°C for 10 min. Data represent averages of three independent experiments (mean $\pm$ SEM, * indicates $P<0.05$, ** indicates $P<0.01$ by student's t-test). The ORF of the genes and the regions amplified by the primer pairs are indicated. **(d)** Pol II protein level is comparable in WT and H2A-Y58F yeasts. Whole cell extracts from WT (LPY17876) or H2A-Y58F (LPY17878) yeasts were immunoblotted as indicated. **(e, f)** H2A-Y58F mutation affects transcription. **(e)** WT H2A (LPY17876), H2A-Y58F (LPY19806) and H2A-Y58F H2AZ-Y65F (LPY19894) yeasts, and **(f)** WT (LPY5), and *htz1Δ* strains (LPY11654) transformed with vector (pRS314), *HTZ1* (pLP2252) or *htz1-Y65F* (pLP3200) were grown at 30°C or shifted to 37°C for 10min, RNA was extracted, and transcript levels of the indicated genes were measured by RT-qPCR and normalized to *SCR1,* a Pol III transcript. Data represent technical triplicates of three independent experiments (mean $\pm$ SEM, * indicates $P<0.05$, ** indicates $P<0.01$ as determined by student's t-test). **(g)** Y57 in H2A is phosphorylated during transcriptional elongation. 293T cells were treated with vehicle (DMSO) or flavopiridol (FP) (1 µM) for 4 ½ hr, or treated with FP for 4 ½ hr, then FP was washed out and harvested at the indicated times, and nuclear extracts were immunoblotted as indicated. Each lane is an independent biological sample.

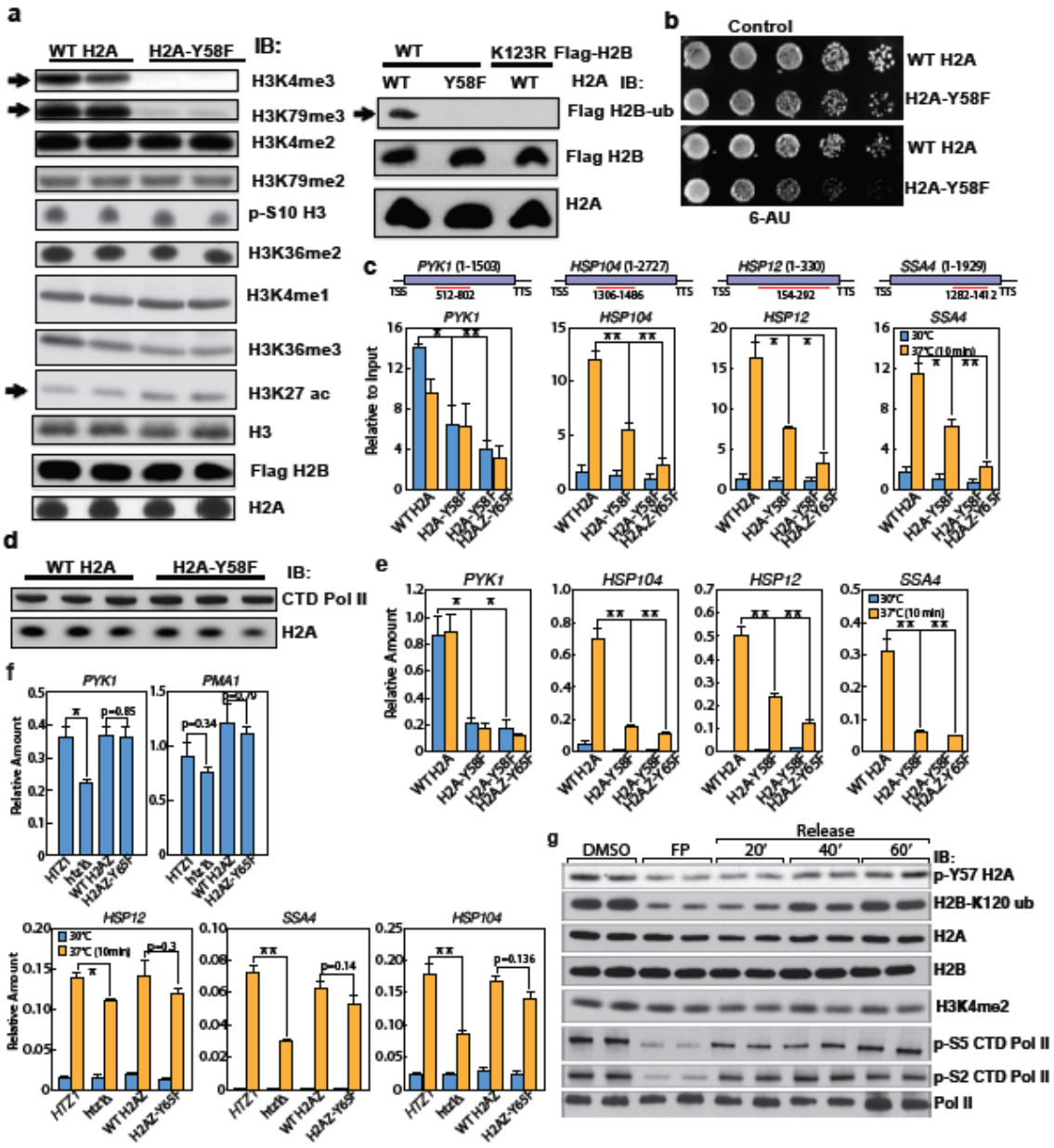
a
WT H2A
H2A-Y58F
IB:
H3K4me3
H3K79me3
H3K4me2
H3K79me2
p-S10 H3
H3K36me2
H3K4me1
H3K36me3
H3K27 ac
H3
Flag H2B
H2A
WT
K123R
Flag-H2B
WT
Y58F
WT
H2A IB:
Flag H2B-ub
Flag H2B
H2A
b
Control
WT H2A
H2A-Y58F
WT H2A
H2A-Y58F
6-AU
c
PYK1 (1-1503)
512-802
HSP104 (1-2727)
1306-1486
HSP12 (1-330)
154-292
SSA4 (1-1929)
1282-1412
TSS
TTS
PYK1
HSP104
HSP12
SSA4
Relative to Input
30°C
37°C (10 min)
WT H2A
H2A-Y58F
H2A-Y58F H2AZ-Y65F
d
WT H2A
H2A-Y58F
IB:
CTD Pol II
H2A
e
PYK1
HSP104
HSP12
SSA4
Relative Amount
30°C
37°C (10 min)
f
PYK1
PMA1
HSP12
SSA4
HSP104
Relative Amount
p=0.85
p=0.34
p=0.3
p=0.14
p=0.136
HTZ1
htz1Δ
WT H2AZ
H2AZ-Y65F
g
DMSO
FP
Release
20′
40′
60′
IB:
p-Y57 H2A
H2B-K120 ub
H2A
H2B
H3K4me2
p-S5 CTD Pol II
p-S2 CTD Pol II
Pol II

Chapter 5. H2A-Y57/58 phosphorylation regulates DNA damage repair

One of the histone modifications affected by H2A-Y58F mutation was Ser128 phosphorylation in H2A, which was increased in the H2A-Y58F yeast **(Fig. 7a)**. This phosphorylation increases during DNA damage, and is a highly conserved hallmark of DNA damage[9]. An increase in phosphorylation thus suggests a defective DDR program in the H2A-Y58F yeast. We investigated if the mutant yeast is more sensitive to DNA damaging agents using ultra-violet (UV) rays and hydroxyurea (HU) as inducers of DNA damage. Indeed, the H2A-Y58F mutant yeast was sensitive to the DNA damaging agents **(Fig. 7b)**. Next, we tested if similar effects are observed in mammalian cells. In mammals, the residue corresponding to Ser128 in yeast is present only in the H2AX variant of H2A (Ser139). We reconstituted *H2AX-/-* MEFs with either WT or H2AX-Y57F, and checked the level of Ser139 phosphorylation in H2AX (referred as γH2AX). DNA damage was induced by treating cells with gamma irradiation, and γH2AX level was monitored by immunoblotting. Both WT and H2AX-Y57F cells showed an increase in the level of γH2AX after irradiation. However, only the cells reconstituted with H2AX-Y57F retained high levels of γH2AX 10 hours post irradiation **(Fig. 7c),** suggesting higher levels of DNA damage in H2AX-Y57F cells. This result suggests a role for H2AX-Y57 phosphorylation in the DDR program in mammals. Next, we tested if H2A-Y57 phosphorylation changes following DNA damage. We observed a decrease in H2A-Y57 phosphorylation post-irradiation, and the phosphorylation returned to normal level 6 hours post

irradiation **(Fig. 7d)**. Collectively, these results suggest that H2A-Y57/58 phosphorylation is necessary for normal DNA damage repair process.

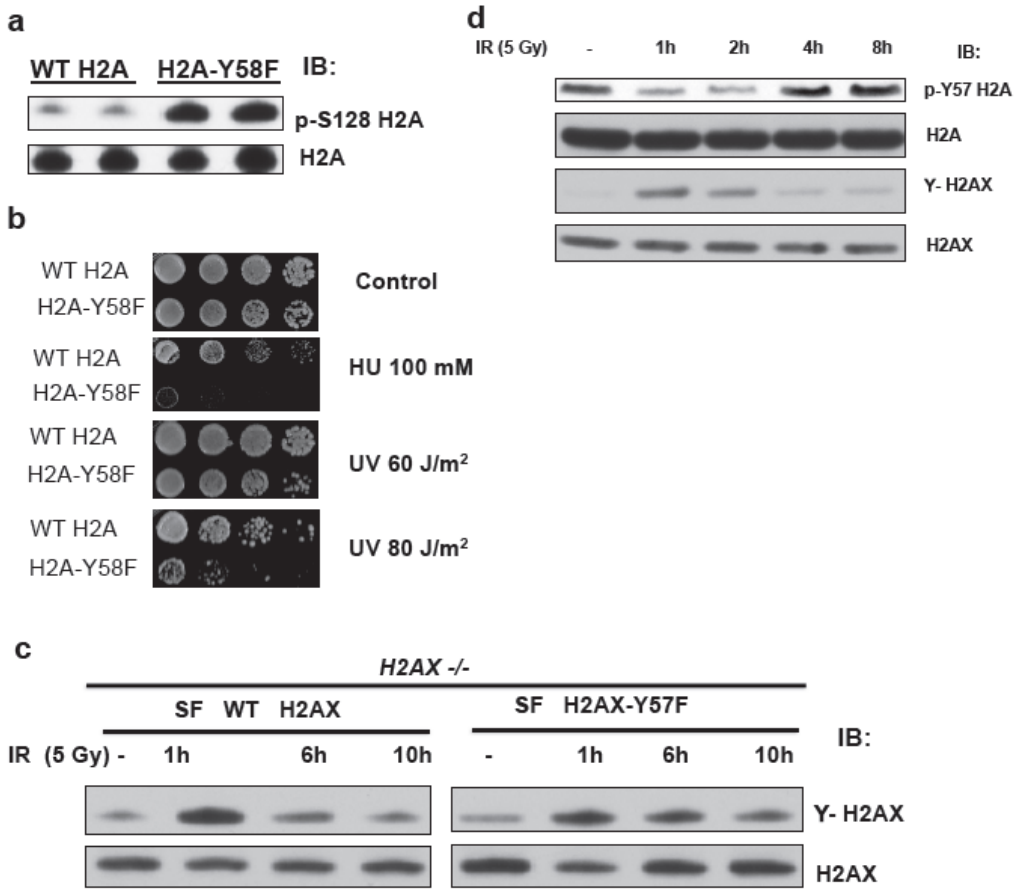

Figure 7. H2A-Y57/58 phosphorylation regulates DNA damage repair. (a, b) H2A-Y58F mutant yeast has defective DNA damage repair system. **(a)** H2A-Y58F yeast has higher level of DNA damage indicative γH2AX mark. Whole cell extracts from WT (LPY17876) and H2A-Y58F (LPY17878) strains were immunoblotted as indicated. Each lane is an independent biological sample. **(b)** Five-fold serial dilutions of WT (LPY18192) and H2A-Y58F (LPY18194) cells were plated on SC supplemented with 100 mM Hydroxyurea (HU) or treated with indicated dose of Ultra violet (UV) light. **(c, d)** H2A-Y57 phosphorylation is involved in DNA damage repair in mammals. **(c)** *H2AX-/-* MEFs were reconstituted with SF-WT H2AX or SF-H2AX-Y57F, irradiated (IR) with 5 Gy dose, and kinetics of γ-H2AX was monitored by immunoblotting as indicated. **(d)** 293T cells were irradiated with 5 Gy IR, and kinetics of the indicated H2A/H2AX modifications were monitored by immunoblotting with the indicated antibodies.

Chapter 6. H2A-Y58F mutation enhances H2B deubiquitylation by SAGA complex

We investigated the mechanism through which H2A-Y58 phosphorylation regulates H2B ubiquitylation. It is possible that the phosphorylation facilitates the ubiquitylation process or prevents the deubiquitylation events. In yeast, H2B is ubiquitylated by the Rad6/Bre1 ubiquitin ligase, and the Paf1 protein complex is required for creating the ubiquitylation whereas *UBP8* deubiquitylates H2B during transcriptional elongation. We first determined whether the recruitment of some of the components known to be involved in H2B ubiquitylation is impaired in the H2A-Y58F yeast by ChIP-qPCR. We found that the binding of Paf1 and Rtf1 was comparable in both WT and H2A-Y58F yeast whereas the binding of Rad6 was slightly reduced in the H2A-Y58F yeast in the tested genes **(Fig. 8a-c)**. The protein levels of Paf1, Rtf1, and Rad6 were comparable in both WT and the H2A-Y58F yeast as detected by immunoblotting **(Fig. 8a-c)**.

Next, we tested if the phosphorylation is preventing the deubiquitylation event. We checked the level of H2B mono-ubiquitylation in the *UBP8*-deleted strain. Intriguingly, the deletion of *UBP8* restored the defect in H2B mono-ubiquitylation in the H2A-Y58F yeast **(Fig. 8d)**. To our great surprise, we found that the restoration of H2B mono-ubiquitylation only partially rescued the defect in H3K79me3, and H3K4me3 remained low in the H2A-Y58F yeast **(Fig. 8d)**. This result was unexpected because several studies have previously reported that H2B mono-ubiquitylation regulates H3K4me3 and H3K79me3[52,96]. However, our result is consistent with a recent report suggesting that H2B mono-

ubiquitylation-creating machinery is important for the establishment of H3K4me3 and H3K79me3, not the H2B mono-ubiquitylation itself[97]. Our result also demonstrates that the H2B ubiquitylation machinery is functional in the H2A-Y58F yeast, and the mutation is regulating DUB activity and not ubiquitylation activity.

We tested if the restoration of the H2B mono-ubiquitylation rescues the defect in transcriptional elongation observed in the H2A-Y58F yeast. We checked Pol II binding in actively transcribed genes by ChIP-qPCR in two constitutively active genes, *PYK1* and *PMA1*, and found that Pol II binding was still reduced in the H2A-Y58F yeast with *UBP8* deletion **(Fig. 8e)**. Likewise, the transcripts of the corresponding genes also showed similar patterns **(Fig. 8f)**. In addition, *UBP8* deletion did not rescue the defect in growth in the H2A-Y58F yeast **(Fig. 8g)**. Collectively these results suggest that the physiological effects of H2A-Y58 mutation are linked to, but extend beyond, the loss of H2B monoubiquitylation.

Chapter 6, in part, has been accepted for publication of the material as it may appear in *Nature* 2014. Basnet, Harihar; Su, Xue B.; Tan, Yuliang; Meisenhelder, Jill; Merkurjev, Daria; Ohgi, Kenneth A.; Hunter, Tony; Pillus, Lorraine & Rosenfeld Michael G. Nature Publishing Group. 2014. The dissertation author was the primary investigator and author of this paper.

Figure 8. H2A-Y58F mutation enhances H2B deubiquitylation by SAGA complex. (a- c) The H2A-Y58 mutation has moderate to no effect on the recruitment of the H2B ubiquitylation machinery. Binding of **(a)** Rtf1-HA, **(b)** Paf1-Myc, and **(c)** Rad6-HA was measured by ChIP-qPCR using tagged strains mentioned in the Yeast strains list. Expression of the tagged proteins was verified by immunoblotting. ORFs of the genes, and the regions amplified by the primer pairs are indicated. **(d)** SAGA complex component (*UBP8*) deletion rescues the defect in H2B mono-ubiquitylation in the H2A-Y58F yeast mutant. Whole cell extracts from WT H2A *UBP8* (LPY16267), H2A-Y58F *UBP8* (LPY16269), WT H2A *ubp8Δ* (LPY16563), H2A-Y58F *ubp8Δ* (LPY16565), and H2B-K123R *ubp8Δ* (LPY18606) strains were immunoblotted as indicated. Each lane is an independent biological sample. **(e-g)** Restoration of H2B mono-ubiquitylation is not sufficient to rescue defects in transcriptional elongation and growth observed in H2A-Y58F yeast. **(e)** *UBP8* deletion does not rescue Pol II binding in the H2A-Y58F mutant. Pol II binding in the WT H2A *UBP8* (LPY16267), H2A-Y58F *UBP8* (LPY16269), WT H2A *ubp8Δ* (LPY16563) and H2A-Y58F *ubp8Δ* (LPY16565) strains were measured by ChIP-qPCR. Data represent triplicates of three independent experiments (mean $\pm$ SEM, * indicates $p<0.05$, ** indicates $p<0.01$ as determined by student's t-test). The ORF of the indicated genes and the regions amplified by the primer pairs are indicated. **(f)** *UBP8* deletion does not rescue the defect in transcriptional output in the H2A-Y58F yeast. The mRNA levels of the indicated genes were determined by RT-qPCR and normalized to *SCR1* transcript. Data represent triplicates of two independent experiments (mean $\pm$ SEM). **(g)** *UBP8* deletion does not rescue the growth defect in the H2A-Y58F yeast. *UBP8* (KY1600) and *ubp8Δ* strains (KY2248) transformed with WT H2A or H2A-Y58F were plated at 2.5-fold serial dilutions on SC-His-Ura for growth and 5-FOA for the removal of pJH33.

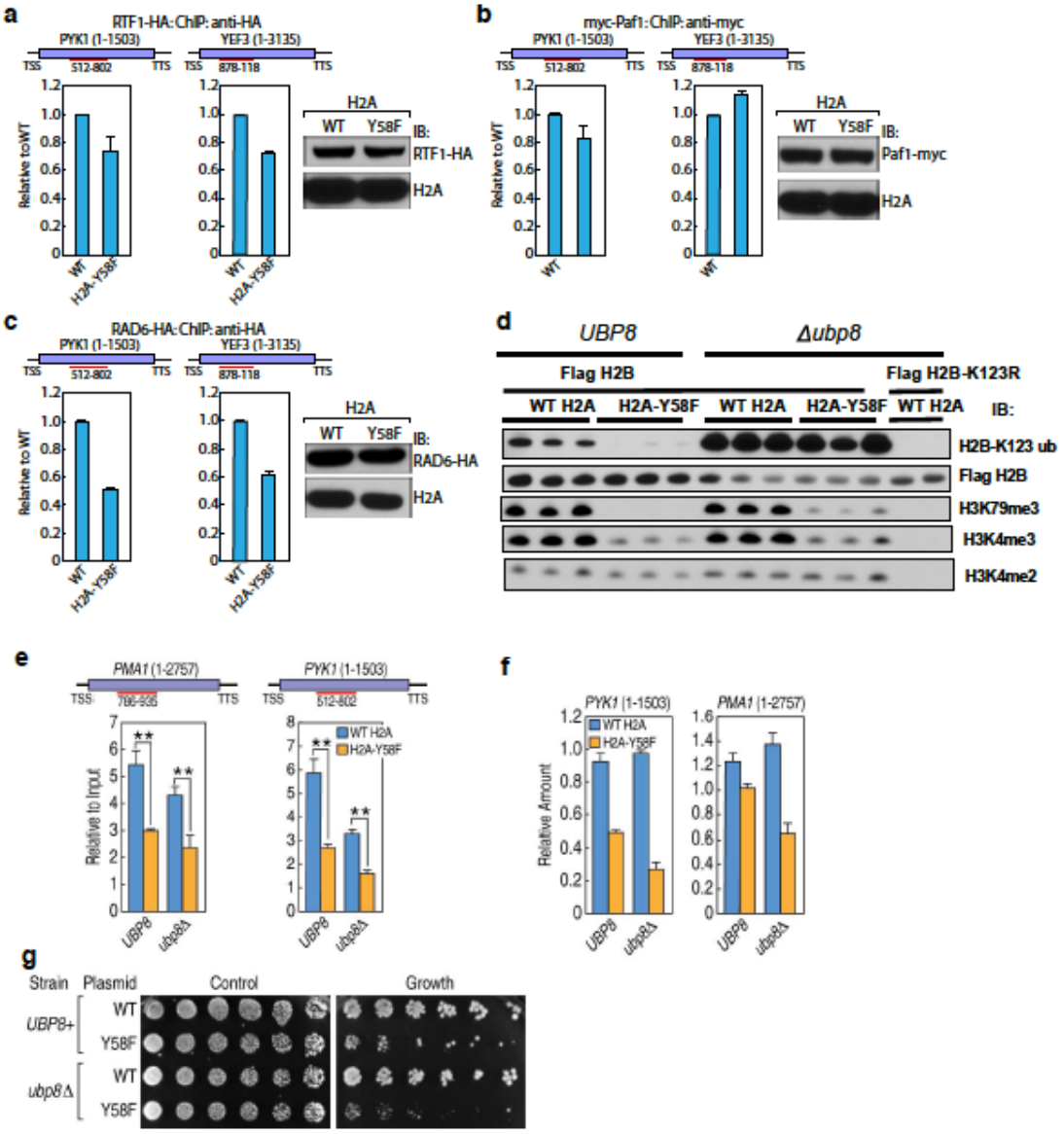
a
RTF1-HA: ChIP: anti-HA
PYK1 (1-1503)
YEF3 (1-3135)
TSS
512-802
TTS
878-118
Relative to WT
WT
H2A-Y58F
H2A
WT
Y58F
IB:
RTF1-HA
H2A
b
myc-Paf1: ChIP: anti-myc
Paf1-myc
c
RAD6-HA: ChIP: anti-HA
RAD6-HA
d
UBP8
Δubp8
Flag H2B
Flag H2B-K123R
WT H2A
H2A-Y58F
IB:
H2B-K123 ub
Flag H2B
H3K79me3
H3K4me3
H3K4me2
e
PMA1 (1-2757)
786-935
Relative to Input
WT H2A
H2A-Y58F
UBP8
ubp8Δ
f
Relative Amount
g
Strain
Plasmid
Control
Growth
UBP8+
ubp8Δ
WT
Y58F

Chapter 7. CK2 phosphorylates the Y57 residue in H2A, and prevents H2B deubiquitylation.

The next question was which protein kinase phosphorylates Y57/Y58 residue in H2A. One of the several approaches that we employed to identify the potential kinase responsible for the phosphorylation of H2A-Y57 residue was to identify the proteins that interact with either WT or H2AX-Y57F. Enzymes and substrates have to interact specifically during reaction, so in some cases it is possible to identify the kinase for a substrate of interest by co-immunoprecipitation[11]. We expressed Flag-tagged WT and H2AX-Y57F in 293T cells, immunoprecipitated H2AX, and identified the interacting proteins by mass spectrometry. We found that casein kinase 2 (CK2)α, the catalytic subunit of CK2, preferentially interacts with H2AX-Y57F. This interaction was verified by immunoblotting, which showed an increased interaction of CK2α with H2AX-Y57F compared to the WT **(Fig. 9a)**. CK2 is an attractive H2A-Y57 kinase candidate as it is one of the few kinases conserved from yeast to mammals with tyrosine phosphorylation activity. Although CK2 most commonly phosphorylates serine/threonine, there are a couple of cases where it has been shown to phosphorylate tyrosine[98,99], establishing it as a dual-specificity kinase. We first tested if CK2α can phosphorylate Y57 residue in H2A *in vitro*. Histone modifications can occur in free histones or in histones assembled into nucleosomes[11,39,40,62,100]. We expressed WT and H2AX-Y57F in 293T cells, purified full-length H2AX or nucleosomal H2AX, and used them as substrates in

a kinase reaction. GST-tagged CK2α expressed in *E. coli* was used as kinase. We found that the CK2α phosphorylate Y57 residue in H2AX preferentially in the context of nucleosomes **(Fig. 9b)**. The phosphorylation was inhibited by a specific CK2 inhibitor, TBBz[101]. To firmly establish the tyrosine phosphorylation activity of CK2α on H2AX in the context of nucleosome, a kinase reaction was performed using recombinant CK2α, WT or H2AX-Y57F containing nucleosome and γ^{32}P ATP, and then phosphoamino acid analysis (PAA) of phosphorylated H2AX was performed. This experiment revealed the tyrosine phosphorylation activity of CK2 on WT H2AX, and the phosphorylation was reduced in H2AX-Y57F **(Fig. 9c)**. In addition, it also revealed that CK2α phosphorylates serine and tyrosine but not threonine in H2AX. Collectively, these results demonstrate that CK2 can phosphorylate Y57 residue in H2A *in vitro*.

We next examined if CK2 phosphorylates H2A-Y57 *in vivo*. H2A-Y57 phosphorylation was decreased upon CK2α knockdown in 293T cells **(Fig. 9d)**. Likewise, H2A-Y57 phosphorylation showed a dose-dependent decrease in response to TBBz in 293T cells **(Fig. 9e)**. Collectively, these results demonstrate that CK2 phosphorylates the Y57 residue in H2A both *in vivo* and *in vitro* in the context of nucleosomes.

Since H2A-Y58 mutation showed a decrease in H2B mono-ubiquitylation, we tested if CK2α knockdown and CK2 inhibition also result in a decrease in H2B mono-ubiquitylation. As expected, we observed a decrease in H2B mono-ubiquitylation in both cases **(Fig. 9d, e)**. We also tested if the decrease in H2B

mono-ubiquitylation is through *UBP8*. Indeed, we observed that H2B mono-ubiquitylation was decreased in WT yeast but not in *UBP8*-null yeast upon TBBz treatment **(Fig. 9f)**. Collectively, these results demonstrate that CK2 regulates H2B mono-ubiquitylation by preventing deubiquitylation through Y57 phosphorylation.

Chapter 7, in part, has been accepted for publication of the material as it may appear in *Nature* 2014. Basnet, Harihar; Su, Xue B.; Tan, Yuliang; Meisenhelder, Jill; Merkurjev, Daria; Ohgi, Kenneth A.; Hunter, Tony; Pillus, Lorraine & Rosenfeld Michael G. Nature Publishing Group. 2014. The dissertation author was the primary investigator and author of this paper.

Figure 9. CK2 phosphorylates the Y57 residue in H2A, and prevents H2B deubiquitylation. **(a)** CK2α interacts preferentially with the H2A-Y57F mutant. Flag-tagged WT and H2AX-Y57F were expressed in 293T cells, and nuclear extracts were co-immunoprecipitated with anti-Flag antibody and immunoblotted as indicated. **(b, c)** CK2 phosphorylates the Y57 residue in H2A in nucleosomes *in vitro.* **(b)** *In vitro* kinase assays were performed using recombinant GST-CK2α and indicated full-length or nucleosomal Flag-tagged H2AX purified from 293T cells in the presence or absence of TBBz, and were immunoblotted as indicated. **(c)** An *in vitro* kinase reaction was performed using recombinant CK2α, 10 μCi of γ^{32}P labeled ATP supplemented with 10 μM cold ATP, and nucleosomes containing Flag-tagged WT or H2AX-Y57F from 293T cells, and PAA of the Flag-tagged H2AX was performed. The red circle indicates phospho-Ser, the blue circle indicates phospho-Thr and the green circle indicates phospho-Tyr. **(d, e)** CK2 phosphorylates the Y57 residue in H2A *in vivo.* **(d)** CK2α was knocked down in 293T cells, and nuclear extracts were immunoblotted with the indicated antibodies. **(e)** CK2 was inhibited in 293T cells for 3 hr with the indicated concentrations of TBBz, and nuclear extracts were immunoblotted as indicated. **(f)** CK2 prevents the deubiquitylation of H2B. WT or *ubp8Δ* cells were treated with vehicle (DMSO) or TBBz (25 μM) for 3 hr and whole cell extracts from the cells were immunoblotted with the indicated antibodies.

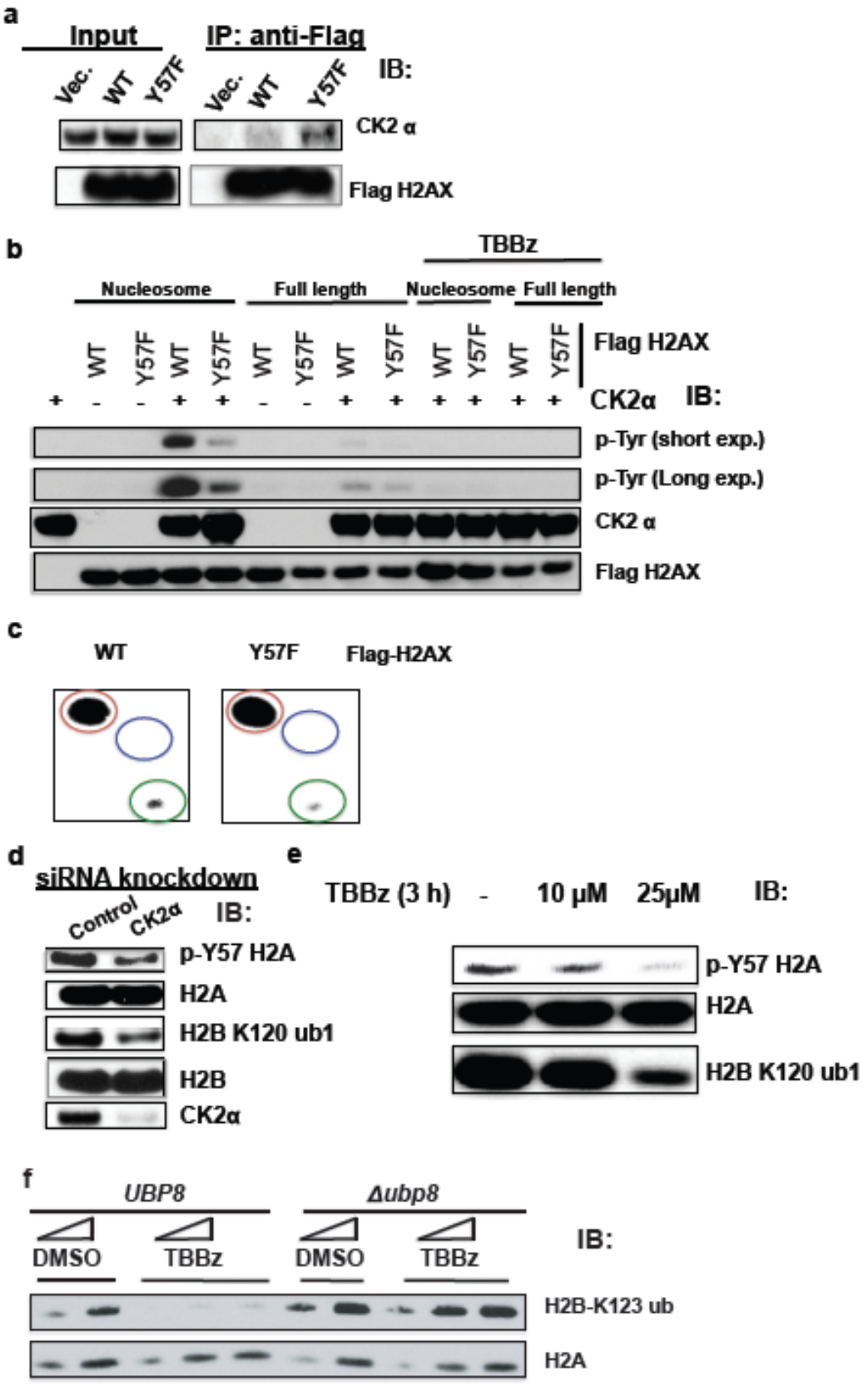
a
Input
IP: anti-Flag
Vec.
WT
Y57F
Vec.
WT
Y57F
IB:
CK2 α
Flag H2AX
b
TBBz
Nucleosome
Full length
Nucleosome
Full length
WT
Y57F
WT
Y57F
WT
Y57F
WT
Y57F
WT
Y57F
WT
Y57F
WT
Y57F
Flag H2AX
CK2α
IB:
p-Tyr (short exp.)
p-Tyr (Long exp.)
CK2 α
Flag H2AX
c
WT
Y57F
Flag-H2AX
d
siRNA knockdown
Control
CK2α
IB:
p-Y57 H2A
H2A
H2B K120 ub1
H2B
CK2α
e
TBBz (3 h)
-
10 μM
25μM
IB:
p-Y57 H2A
H2A
H2B K120 ub1
f
UBP8
Δubp8
DMSO
TBBz
DMSO
TBBz
IB:
H2B-K123 ub
H2A

Chapter 8. CK2 positively regulates transcriptional elongation in actively transcribed genes

Since H2A-Y58F mutation led to a defect in transcriptional elongation, we determined if CK2 inhibition would exhibit a similar defect in transcriptional elongation. For this, we examined the binding of Pol II in LNCaP prostate carcinoma cells treated with TBBz by ChIP-sequencing (ChIP-seq). TBBz treatment resulted in a decrease in Pol II binding in the gene bodies of actively transcribed genes **(Fig. 10a)**. In contrast, the binding in the promoter region was not affected by TBBz treatment **(Fig. 10a).** The Pol II binding profile in CK2-inhibited cells was very similar to promoter proximal pausing phenomena[102,103]. We plotted the traveling ratio (TR) plot of Pol II[102,103], which is the ratio of the Pol II density in the promoter to the density in the gene body, to determine whether CK2 plays an important role in promoter proximal pausing. Indeed, CK2-inhibited cells showed an obvious shift in the TR plot **(Fig. 10a),** suggesting that CK2 kinase activity is required for the transition of Pol II from the initiation to the elongation stage. Likewise, in agreement with the role of CK2 in transcriptional elongation, dihydrotestosterone (DHT)-induced transcriptional activation of androgen receptor (AR)-regulated genes was impaired or abolished in LNCaP cells treated with TBBz as determined by RT-qPCR **(Fig. 10b).** Collectively, these data demonstrate that CK2 is a crucial positive regulator of transcriptional elongation.

We sought to understand the molecular details of the role of CK2 in transcriptional elongation by determining its genome-wide localization in LNCaP cells by ChIP-sequencing. Like Pol II, CK2α showed binding to actively transcribed genes across gene bodies, although its binding profile was somewhat distinct from that of Pol II **(Fig. 10c)**. Meta analysis of the top 10% most active genes, based on Gro-seq results in LNCaP cells[104], revealed that CK2α globally co-localizes with Pol II **(Fig. 10d)**. Consistent with the genome-wide binding pattern of CK2α, Ser-5 phosphorylated CTD of Pol II, which is localized in the 5' region of actively transcribed genes, and Ser-2 phosphorylated CTD of Pol II, which is localized in the gene bodies and 3' region of actively transcribed genes, both co-immunoprecipitated with CK2α **(Fig. 10e)**. Collectively, these results indicate that CK2 globally regulates transition from the initiation to the elongation stage during transcription.

Next, we asked if CK2 also regulates transcriptional elongation in yeast, and if so, whether H2A-Y58 phosphorylation is a key player, among the many other substrates of CK2[105], in this regulation. Inhibition of CK2 activity by TBBz resulted in the decreased recruitment of Pol II to two constitutively active genes, *PYK1* and *PMA1*, in both the promoter region as well as gene bodies in the WT yeast **(Fig. 10f)**. The removal of TBBz reversed the defect of Pol II binding **(Fig. 10f)**. On the other hand, TBBz did not have any additive effect in decreasing Pol II binding in the H2A-Y58F mutant yeast **(Fig. 10f)**, suggesting that H2A-Y58 phosphorylation is a critical event in CK2-mediated regulation of transcriptional

elongation. It is noteworthy that both CK2 inhibition and mutation of H2A-Y58 did not result in promoter proximal pausing in the genes tested, which is consistent with the observation that regulation by promoter proximal pausing is rare in yeast[106]. Collectively, these results demonstrate that CK2 plays a deeply conserved role in transcriptional elongation in gene bodies, and that H2A-Y58 phosphorylation is critical in this regulation.

Chapter 8, in part, has been accepted for publication of the material as it may appear in *Nature* 2014. Basnet, Harihar; Su, Xue B.; Tan, Yuliang; Meisenhelder, Jill; Merkurjev, Daria; Ohgi, Kenneth A.; Hunter, Tony; Pillus, Lorraine & Rosenfeld Michael G. Nature Publishing Group. 2014. The dissertation author was the primary investigator and author of this paper.

Figure 10. CK2 regulates transcriptional elongation in actively transcribed genes. (a) CK2 kinase activity is required for promoter-proximal pause release. The traveling ratio of Pol II in active genes in LNCaP cells was plotted for cells treated with DMSO (vehicle) or with TBBz (25 μM) for 2½ hr. Overlay of occupancy of Pol II in vehicle- and TBBz-treated cells in representative active genes (*TMPRSS2* and *NKX3-1*) is shown. **(b)** CK2 kinase activity is necessary for normal gene expression. LNCaP cells were treated with vehicle (DMSO) or TBBz (25 μM) for 60 min, and then treated with vehicle (EtOH) or 100 nM DHT for 90 min, and induction of the indicated AR target genes was measured by RT-qPCR. Data represent triplicates of three independent experiments (mean ± SEM, * indicates $p<0.05$, ** indicates $p<0.01$ determined by student's t-test). **(c, d)** CK2α binds globally across the gene body of actively transcribed genes. **(c)** Occupancy of CK2α and Pol II in the top 10% of active genes (n= 3162) and all genes in LNCaP cells were determined by CEAS[107]. The length of all gene bodies is normalized to 3kb. Enrichment of CK2α and Pol II at a representative active gene (*NKX3-1*) is shown. **(d)** Heat map of the binding profile of Pol II and CK2α in top 10% of active genes in LNCaP cells from Transcription Start Site (TSS) to Transcription Termination Site (TTS) is shown. **(e)** H2A-Y58 phosphorylation is critical for CK2-mediated regulation of transcriptional elongation. WT (LPY17876) and H2A-Y58F (LPY17878) cells were treated with DMSO (vehicle) or TBBz (25 μM) for 3 hr, or treated with TBBz for 3 hr followed by the release of inhibition for 1 hr (TBBz 1 hr R), and Pol II binding in the indicated genes was measured by ChIP-qPCR in WT H2A and H2A-Y58F yeast. Data represent triplicates of three independent experiments (mean ± SEM). The ORF of the genes and the regions amplified by the primer pairs are indicated.

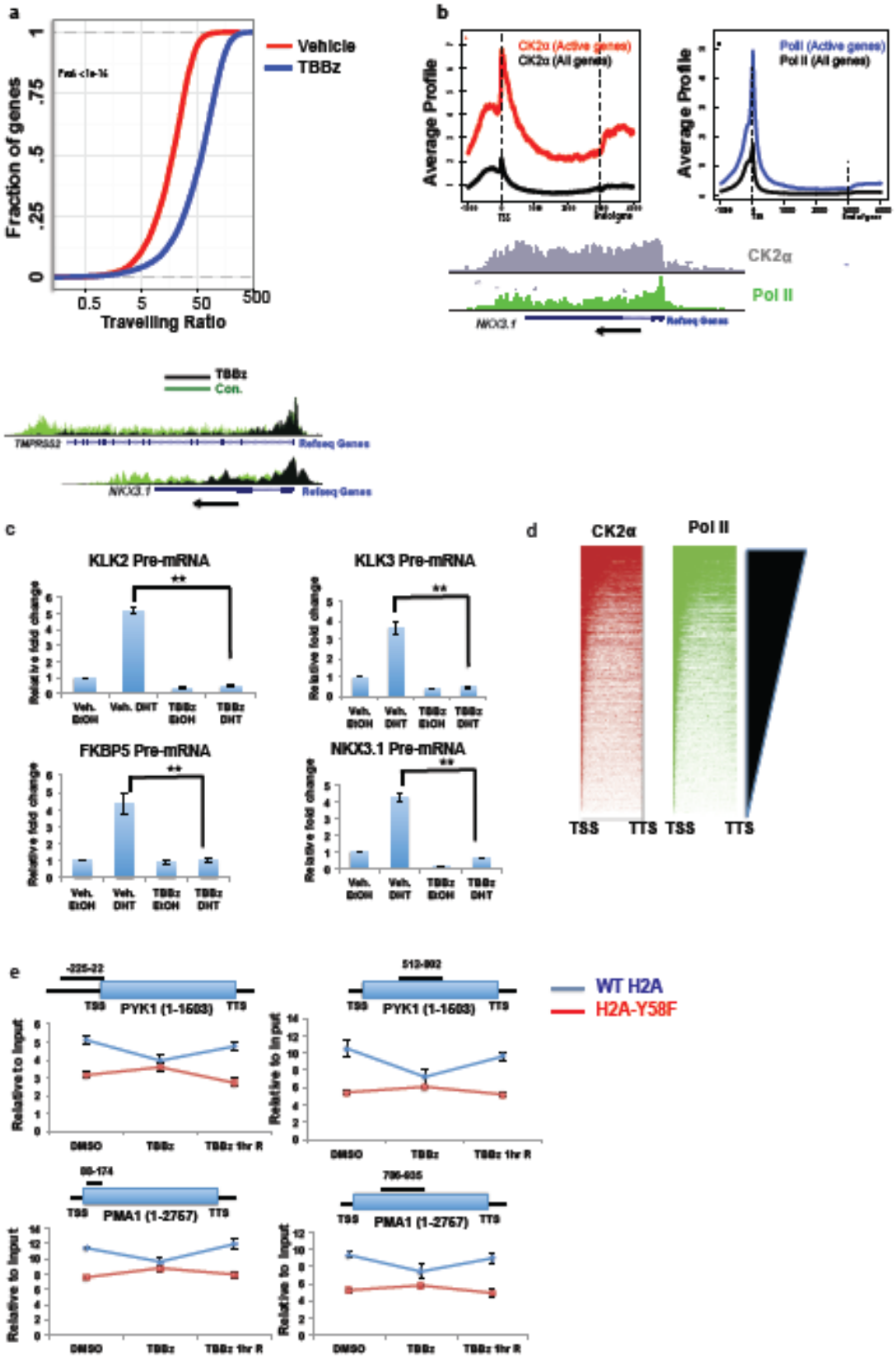
a
Vehicle
TBBz
Fraction of genes
Travelling Ratio
b
CK2α (Active genes)
CK2α (All genes)
Pol II (Active genes)
Pol II (All genes)
Average Profile
CK2α
Pol II
NKX3.1
Refseq Genes
TBBz
Con.
TMPRSS2
c
KLK2 Pre-mRNA
KLK3 Pre-mRNA
FKBP5 Pre-mRNA
NKX3.1 Pre-mRNA
Relative fold change
Veh. EtOH
Veh. DHT
TBBz EtOH
TBBz DHT
d
CK2α
Pol II
TSS
TTS
e
PYK1 (1-1603)
PMA1 (1-2767)
Relative to Input
DMSO
TBBz
TBBz 1hr R
WT H2A
H2A-Y58F

Chapter 9. CK2 binds to active enhancers and regulates transcriptional elongation in enhancers

Although a majority of CK2α binding was observed over gene bodies, we noted some binding sites in the intergenic regions that mostly co-localized with H3K4mono-methyl and H3K27acetyl marks, histone modifications that co-localize with active enhancers[108], suggesting that the intergenic CK2α peaks are in enhancer regions. LNCaP cells have cell-type specific active enhancers that are marked by the binding of AR; hence, we examined the potential co-localization of intergenic CK2α peaks with known AR enhancers. We found that majority of AR enhancers exhibit CK2α binding **(Fig. 11a**). In recent years, it has been reported that there is transcription in active enhancers that produces a class of non-coding RNA called eRNA[104,109–111]. We tested if CK2 inhibition also causes Pol II pausing in enhancers. Pol II tag density in either side of the AR-bound enhancers showed that inhibition of CK2 caused Pol II stalling in the AR-bound enhancers **(Fig. 11b),** underpinning the function of CK2 in transcriptional elongation in enhancers.

Chapter 9, in part, has been accepted for publication of the material as it may appear in *Nature* 2014. Basnet, Harihar; Su, Xue B.; Tan, Yuliang; Meisenhelder, Jill; Merkurjev, Daria; Ohgi, Kenneth A.; Hunter, Tony; Pillus, Lorraine & Rosenfeld Michael G. Nature Publishing Group. 2014. The dissertation author was the primary investigator and author of this paper.

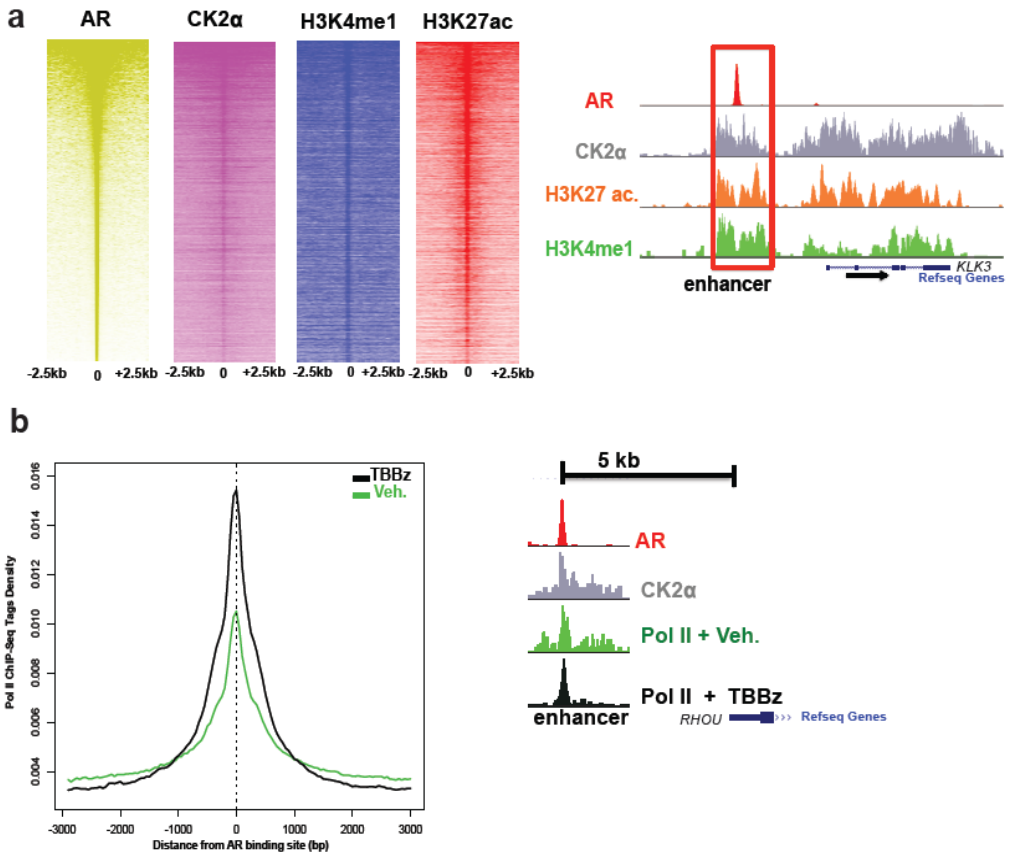

Figure 11. CK2 binds to active enhancers and regulates transcriptional elongation in enhancers. **(a)** CK2α binds to active enhancers. Heat maps of CK2α, H3K4me1[104], and H3K27acetyl[104] signals over Androgen Receptor (AR)[104]-enriched regions in LNCaP cells were determined by CEAS. Enrichment of CK2α, H3K4me1[104], H3K27acetyl[104], and AR[104] at a representative AR enhancer (*KLK3*) is shown. **(b)** CK2 regulates transcriptional elongation in enhancers. Shown is a Pol II ChIP tag density plot centered at AR enriched enhancers. Pol II tag density at a representative *RHOU* enhancer is shown.

Conclusion

In summary, we have identified a highly conserved novel tyrosine phosphorylation in H2A (Y57), mediated by CK2 kinase, that plays a critical role in transcriptional elongation and DNA damage repair by modulating several functionally important post-translational modifications in histones that include H2A-ub, H2B-ub, H3K4me3, H3K79me3, and γ-H2AX, at least in part by antagonizing the activity of the SAGA complex **(Fig. 12)**.

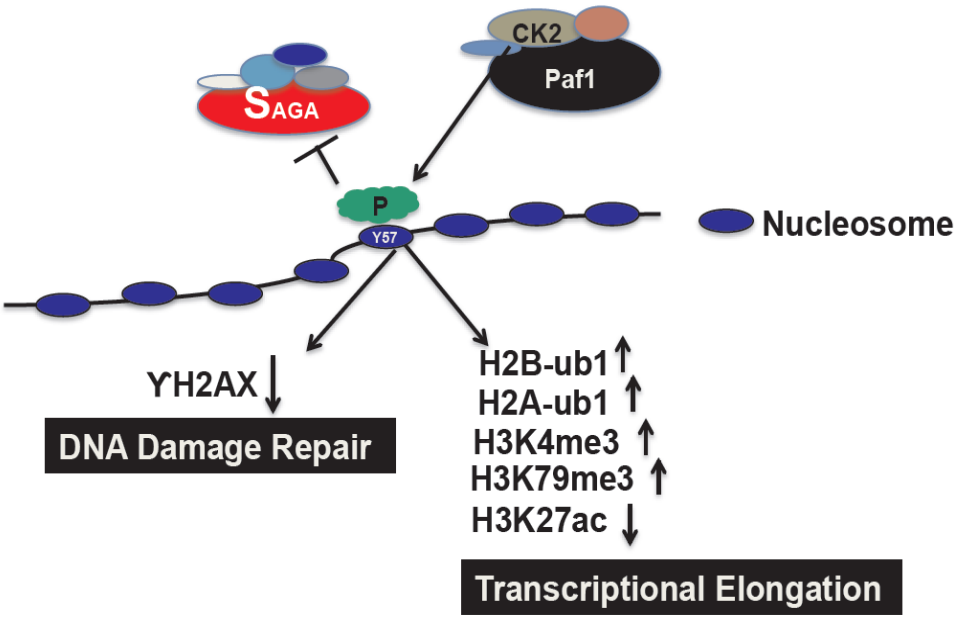

Figure 12. Proposed working model. Proposed working model of the role H2A-Y57 phosphorylation in regulating transcriptional elongation and DNA damage repair by modulating indicated histone modifications, and by antagonizing the SAGA complex activity.

Discussion

Post-translational modifications in histones have been shown to play critical roles in maintaining genomic stability and gene expression. Several studies have done extensive analyses of the role of each amino acid in all four histones by alanine screening[79,112,113]. These studies have categorized all the histone residues by their roles in different biological processes such as DNA damage repair, growth, or transcriptional elongation by testing the sensitivity of the mutants to DNA damaging agents (such as UV and HU) or transcriptional elongation assay (such as 6-AU). Furthermore, one study has identified several residues that are necessary for the establishment of some of the important histone marks like H3K4me3, H3K4me2, and H3K4me1[79]. Our data clearly indicate that mutation of the Y58 residue in H2A causes defects in growth, transcriptional elongation, and DNA damage repair, as well as defects in H3K4me3. Interestingly, the functional role of the Y58 residue has been missed by all these previous studies because the tyrosine residue was substituted with alanine instead of phenylalanine, which causes lethality in yeast. Thus, our study has identified a very important functional role of Y58 residue in H2A that was overlooked in previous studies. Intriguingly, the regulation occurs through phosphorylation of the residue, establishing the Y57/58 phosphorylation as one of the most important histone modifications identified so far. An improvement in histone alanine scanning studies, specially of residues that might be potentially modified, by replacing the residue with structurally more conservative amino

acids might yield some new information about the potential role of the histone residues, and thus the modifications in some cases.

Another interesting discovery made in our study is the identification of CK2 as the kinase responsible for the phosphorylation. CK2 is a pleiotropic kinase involved in the regulation of cell cycle, DNA damage repair, cell differentiation, and transcription[105]. This kinase is primarily known to phosphorylate serine and threonine, though there is evidence for the tyrosine phosphorylation activity of CK2 *in trans* in a yeast protein called Fpr3[99]. Likewise, there is also a report showing that CK2 can auto-phosphorylate tyrosine *in cis*[98]. However, these tyrosine phosphorylations do not seem to have a functional significance. Due to a lack of clear functional significance, the role of CK2 as a tyrosine kinase has been underappreciated. Our study clearly indicates that CK2-mediated tyrosine phosphorylation of H2A-Y57/Y58 has important functional significance in transcriptional elongation and DNA damage repair. Our study thus invites a search for other potential tyrosine substrates of CK2 that might be important mediators of CK2 function. It is also interesting that CK2 phosphorylates the Y57 residue in the context of nucleosomes. CK2 is known to be an acidophilic kinase[114], and the Y57 residue in H2A is located in the highly conserved acidic patch in the nucleosomes. It is possible that the acidic residues in the nucleosome might be crucial for the phosphorylation, though it cannot be ruled out that other histone modifications or other residues present in the nucleosome might be important for the phosphorylation.

Another important finding of our study is the role of H2A-Y58 phosphorylation in antagonizing the activity of the highly conserved SAGA complex. Transcription is a highly coordinated process that is regulated in each step of initiation, elongation, and termination by multi-protein complexes. One important event during transcriptional elongation is the dynamic change in H2B mono-ubiquitylation at Lys 123, which is established by Paf1/ Rad6/ Bre1, and deubiquitylated by the SAGA complex. Interestingly, both the ubiquitylation and deubiquitylation are required for normal transcriptional output, and both the Paf1 complex and the SAGA complex are localized in the same region in the genome. It remains unclear how the activities of these two highly conserved complexes with opposing enzymatic activity on H2B ubiquitylation are coordinated. This study has identified H2A-Y58 phosphorylation as a modification that antagonizes SAGA complex activity, and that CK2, which interacts with the Paf1 complex[53,115], mediates the phosphorylation. These finding suggests that the Paf1 complex employs CK2 to block the DUB activity of the SAGA complex through H2A-Y58 phosphorylation, and thus maintain H2B mono-ubiquitylation even in the presence of the SAGA complex **(Fig. 12)**. The SAGA complex has also been reported to deubiquitylate H2A in mammals[64]. Hence, it is likely that the defect in H2A mono-ubiquitylation observed in H2A-Y57F in mammalian cells is also through the SAGA complex, though more experiments need to be done to verify such regulation.

Another interesting finding that came out from this study is that contrary to several previous studies, the regulation of H3K4me3 and H3K79me3 is not connected directly to H2B mono-ubiquitylation. In a recent study, it has been shown that deletion of some proteins can specifically affect H2B mono-ubiquitylation without affecting H3K4 and H3K79 methylation[97], which is consistent with our data showing that restoration of H2B mono-ubiquitylation in H2A-Y58F through *UBP8* deletion does not completely rescue the defects in H3K4 and H3K79 methylation. In addition, deletion of *UBP8* in the H2A-Y58F yeast did not rescue the defects in transcriptional elongation and growth. These data indicate that the H2A-Y58 phosphorylation-mediated biology extends beyond the regulation of H2B mono-ubiquitylation. A moderate increase in H3K27 acetylation, which is created by the Gcn5[116] histone acetyl transferase of the SAGA complex, in the H2A-Y58F yeast, suggests that the phosphorylation may antagonize multiple modules of the SAGA complex. Such antagonism could explain the partial rescue of the defects in the H2A-Y58F mutant upon deletion of *UBP8,* as Ubp8 is not required for the integrity of the SAGA complex[55]. More experiments need to be done to test this hypothesis.

Last but not least, identification of the role of CK2 in regulating transcriptional elongation has some important implications as well. So far, the phosphorylation of Ser2 in Pol II CTD mediated by the PTEF b complex is primarily known to regulate the transition from initiation to the elongation step during transcription. This study demonstrates that CK2 kinase activity is also

important in regulating this transition, and suggests the existence of two distinct checkpoints that regulates the transition from transcriptional initiation to elongation, one through the PTEF b complex and another through CK2. More work is required to demonstrate the existence of two distinct checkpoints to regulate the elongation.

Future Directions

This study has demonstrated that the H2A-Y58 phosphorylation regulates the DUB activity of the SAGA complex, and the increase in H3K27ac mark in the H2A-Y58F mutant yeast suggests that the phosphorylation might regulate the acetyl transferase activity of the complex as well. The SAGA complex is a huge 2 MDa complex that consists of more than 15 different proteins[117]. It remains to be identified which component of the SAGA complex interacts with H2A-Y58 phosphorylation. A candidate approach can be taken to identify the component of the SAGA complex interacting with the phosphorylation. Basically, levels of H2B mono-ubiquitylation, H3K4me3, and H3K79me3 can be checked by immunoblotting in the H2A-Y58F yeast in the SAGA component deletion background. If all the defects in the histone modifications are restored, then further experiments can be done to test if the defects in transcriptional elongation, DNA damage repair, and growth can be restored with the deletion. Alternatively, a biochemical approach can be taken to identify the proteins that interact with the H2A-Y57 phosphorylated peptides or nucleosomes containing the phosphorylation as a bait, and identify the interacting proteins. If one or more components of the SAGA complex are found to interact differentially with the phosphorylated and non-phosphorylated H2A-Y57, then the abovementioned genetic experiments can be conducted with the identified proteins.

In this study, we have demonstrated a novel role of CK2 in regulating SAGA complex DUB activity. It remains to be investigated if the CK2 kinase also

affects the acetyl-transferase activity of the SAGA complex mediated by Gcn5. Future studies should test if the recruitment of the components of the SAGA complex is defective in CK2-inhibited cells. Likewise, the level of histone acetylations mediated by the SAGA complex should also be tested in CK2-inhibited cells by ChIP-seq because CK2-mediated phosphorylation/s could regulate SAGA complex activity allosterically instead of through the recruitment process. Furthermore, the role of CK2 in regulating SAGA complex activity should also be tested in the mammalian system as well by inhibiting CK2, and analyzing the recruitment of SAGA complex components as well as acetylated histones by ChIP-seq.

We have also shown that H2A-Y57/58 phosphorylation is involved in DNA damage repair process, though the precise mechanism remains to be elucidated. It is possible that the phosphorylation-mediated regulation of the SAGA complex is involved in the DNA damage repair mediated through H2A-Y57 phosphorylation. However, this needs to be tested. Experiments to check whether the effect of deleting the SAGA complex in H2A-Y58F yeast would relieve the DNA damage sensitivity would yield some useful information on the role of H2A-Y58 phosphorylation in DDR through regulation of the SAGA complex.

Appendix: Materials and Methods

Cell culture, siRNA, Plasmids, Transfection, Antibodies, Kinase inhibitors

LNCaP and 293T cells were cultured in F12 medium supplemented with 10% FBS and glutamine. For the DHT-treatment experiments, LNCaP cells were cultured in Deficient DME High Glucose medium with 5% FBS (charcoal dextran filtered) for 3-4 days. Short interfering RNA (siRNA) against CK2α was purchased from Santa Cruz (sc-29918). Cells were transfected using Lipofectamine 2000 (Invitrogen) using the manufacturer's protocol. Mutagenesis was done using Quikchange Lightening Mutagenesis Kit following the manufacturer's recommended protocol. The following antibodies were used in this study: p-Y57 H2A rabbit antibody was generated by Biomatik Company using phospho-Y57 H2A peptide as an antigen (LE(pY)LTAEILELAGNC), purified, and positively selected using p-Y57 H2A peptide column, and negatively selected using Y57 H2A peptide column; anti-H2A (Abcam Cat. No. ab18255), anti-CK2α (Cat. No. ab 70774), anti-H2B K120 ub (Cell Signaling Cat. No. 5546S), anti-Flag (Sigma M2), anti-RNA polymerase II (Santa Cruz N-20 (for mammalian cells), Abcam Cat. No. ab817 (for yeast cells)), anti-p-Ser2 Pol II (Abcam Cat. No. ab5095), anti-p-Ser5 Pol II (Abcam Cat. No. ab5131), anti-phosphotyrosine (Millipore Cat. No. 05-321 (4G10)), anti-H2A (yeast) (Active Motif Cat. No. 39236), anti-H4K4me3 (Active Motif Cat. No. 39159), anti-H3K4me2 (Millipore Cat. No. 07-030), anti-H3K4me1 (Millipore Cat. No. 07-436), anti-p-S10 H3 (Millipore Cat. No. 06-570), anti-H3K27 acetyl (Abcam Cat. No. ab

4729), anti-H3K79me2 (Active Motif Cat. No. 39924), anti-H3K36me2 (Active Motif Cat. No. 39255) and anti-H2A-K119-ub (Cell Signaling Cat No. 8240S). TBBz and flavopiridol were from Sigma.

Chromatin Immunoprecipitation

Cells were grown to 90-95% confluence, fixed with 1% formaldehyde for 15 min for Pol II ChIP, and with Di-Succinimidyl Glutarate (DSG) for 45 minutes followed by 10 min fixation with 1% formaldehyde for CK2α ChIP. To terminate crosslinking, fixed cells were incubated with glycine (1.25 mM) for 10 min. Nuclei were prepared as described[118], which were then sonicated in lysis buffer (150 mM NaCl, 1% Triton X-100, 20 mM Tris pH 8.0, 0.1% SDS) using a Bioruptor to fragment chromatin to less than 500 bp. Chromatin was pre-cleared with Protein-G magnetic beads, and then immunoprecipitated using 5 µg of antibody per one 10 cm plate for each samples. The chromatin antibody mix was incubated with 35 µl protein G-conjugated Dyna beads for 4 h, washed three times with wash buffer (1% Triton X-100, 50 mM Tris pH 8.0, 10% glycerol) with increasing concentrations of NaCl (150 mM, 300 mM and 400 mM), and two times with Tris-EDTA (TE) buffer. DNA was eluted in 1% SDS, crosslinking was reversed overnight at 65°C, and DNA was purified using Qiagen columns. Yeast ChIP was performed using 300-400 µg DNA and 2 µg antibody using the protocol as described[119] with some modifications. Briefly, cells were fixed for 15 min, and then incubated with glycine at a final concentration of 2.5 mM for 5 min, and cells were lysed using glass beads (5 X 5 minutes beating with 2 min on ice intervals).

Cells were then sonicated to obtain chromatin fragments of less than 1 kb, and the rest of the protocol was similar to the mammalian cells. All the buffers used included fresh complete protease inhibitors (Roche), 1 mM PMSF, 2 mM Na_3VO_4, 10 mM β-glycerol phosphate and 10 mM NaF.

Statistical Analysis

P-values for ChIP-qPCR and RT-qPCR were calculated by Student's T-test, two tails, type two using Microsoft Excel. The statistical significance of the change of Traveling Ratio between control and CK2 inhibitor treated samples was determined using two-tailed K-S test.

Identification of ChIP-seq peaks

ChIP-seq peaks were identified using HOMER (http://biowhat.ucsd.edu/homer). A 200 bp sliding window was used for transcription factors and a 500 bp sliding window was used for histone modifications with the requirement that two peaks are at least 500 bp away for transcription factors, and 1250 bp for histone modifications to avoid redundant peak identification. Tag density was calculated by using HOMER and average signal profiles surrounding AR enriched regions were generated with CEAS[107] (cis-regulatory element annotation system) which were visualized with Java TreeView (http://jtreeview.sourceforge.net).

ChIP-seq Alignment

DNA was ligated to specific adaptors followed by HT sequencing on

Illumina's HiSeq 2000 system according to the manufacturer's instructions. The first 48 bp for each sequence tag returned was aligned to the hg18 (human) assembly using Bowtie2. The data were visualized by preparing custom tracks on the UCSC genome browser by using HOMER. The total number of mappable reads was normalized to 10^7 for each experiment presented.

ChIP-seq Data Deposition

ChIP-seq data has been deposited in GEO. The accession number is: GSE58607.

Traveling Ratio (TR) Calculation

Pol II TR was defined as the relative ratio of Pol II density in the promoter-proximal region and the gene body. The promoter proximal region refers to the window from -50bp to +300bp surrounding transcription start site (TSS), and the gene body refers to regions from 300bp downstream of TSS to 13 kbp from TSS for genes longer than 13kbp, and to the transcription termination site (TTS) for the genes shorter than 13kbp. The significance of the change of TR between control and CK2 inhibitor treated samples was displayed using box plot.

***In vitro* kinase assay and Phosphoamino Acid Analysis (PAA)**

In vitro kinase reactions were performed with 100 ng of recombinant GST-tagged CK2α in 1X kinase buffer (20 mM Tris-HCl, 50 mM KCl, 10 mM $MgCl_2$ pH 7.5) with the addition of 0.2 mM ATP for cold reaction (and 10 μM ATP mixed with 10 μCi of γ^{32}P-labeled ATP for the radioactive reactions). The substrates (Flag-tagged WT H2AX and H2AX-Y57F) were purified from 293T cells

expressing Flag-tagged H2AX constructs. For the full-length proteins, histone extracts were immunoprecipitated using anti-Flag antibody, then washed several times with wash buffer (1% Triton X-100, 900 mM NaCl, 20mM Tris 8.0), treated with CIP for 30 minutes at 37°C, washed few more times with wash buffer, and eluted with 3X Flag peptides. Mononucleosomes were prepared as described[118] with minor changes in micrococcal nuclease digestion. Briefly, nuclei were isolated from 15 cm fully confluent plates, and DNA was digested in 1.2 ml total volume with 2.5 µl micrococcal nuclease (NEB Catalog # M0247S) for 10 minutes at 37 °C, and the reaction was stopped by adding 5 mM EGTA, and mononuclesomes were collected by centrifugation. Mononucleosomes were immunoprecipitated with anti-Flag, washed four times with Buffer A (340 mM Sucrose, 10 mM HEPES pH 7.5, 10% glycerol, 1.5mM $MgCl_2$, 10 mM KCl) followed by three washes with kinase reaction buffer, then treatment with 500 µM FSBA(Sigma cat number F9128-25MG) for 25 min at 37°C to irreversibly inhibit any potential kinases interacting with the nucleosome. Following this were three washes with kinase buffer, treatment with CIP for 30 minutes at 37°C, and another three washes with buffer A. The bound nucleosomes were eluted with 3X Flag peptides in buffer A. The kinase reactions were carried out for 1 hour at 30°C. For PAA, the samples were separated by SDS-PAGE, transferred to PVDF membrane, and the membrane corresponding to the mobility of phosphorylated H2AX was excised, and PAA using two-dimensional electrophoresis on thin layer cellulose plates was performed as described[120].

Whole cell extracts (WCE), Immunoprecipitation (IP) and Cell Fractionation

Yeast whole cell extracts were prepared either by breaking the cells with glass beads in PBS or boiling the cells in denaturing buffer (2% SDS with 30 mM DTT) for 10 min. To immunoprecipitate the Flag-tagged proteins under denaturing conditions in yeast, WCE were prepared as mentioned above in denaturing buffer, and the SDS concentration was adjusted to 0.1% by adding dilution buffer (150 mM NaCl, 1% Triton X-100, 20 mM Tris pH 8.0.), then immunoprecipitated overnight using Flag antibody (M2-Sigma) conjugated to agarose beads, and washed three times with dilution buffer. Bound proteins were eluted with 100 µg/mL 3X Flag peptides in TBS for 30 min at 8°C twice and the eluted proteins were precipitated using Tricholoroacetic acid (TCA). In 293T cells, WCE for denaturing IP was prepared by boiling the cells in lysis buffer (1% SDS, 20 mM Tris pH 8.0, 10 mM DTT), and the SDS concentration was adjusted to 0.1% by adding dilution buffer before adding the Flag antibody for IP. Nuclear extracts were prepared using lysis buffer (10 mM HEPES pH 8.0, 1.5 mM $MgCl_2$, 10 mM KCl, 1% NP40) to lyse cell membrane; the supernatant is the cytosolic fraction and the pellet is the nuclear fraction. For co-IP, the nuclear pellet was re-suspended in lysis buffer (0.1% NP40, 150 mM NaCl, 20 mM Tris pH 8.0 and 10% glycerol), and sonicated to break the nuclei and chromatin. The antibody and nuclear extract were incubated overnight with 5 µg of CK2α antibody or 20 µl of M2 Flag antibody conjugated to magnetic beads. The beads were washed

three times with the same lysis buffer, and the proteins bound to the beads were analyzed by MS or by immunoblotting.

Recombinant protein purification

GST-CK2α was sub-cloned in PGex 6P1 vector, and the protein was expressed in BL21 *E. coli* by inducing with 0.2 mM IPTG for 3 hours at 30°C. For the protein purification, cells were lysed in lysis buffer (20 mM Tris pH 8.0, 300 mM NaCl, 10% glycerol) supplemented with 1% Triton X-100, 1 mg/ml lysozyme for 1 hour at 4°C, followed by sonication. Protein was precipitated using Agarose-glutathoine beads, and eluted with 10 mM reduced glutathione.

Mass Spectrometry

Protein samples were prepared as described[121]. Briefly, the protein samples were diluted in TNE (50 mM Tris pH 8.0, 100 mM NaCl, 1 mM EDTA) buffer. RapiGest SF reagent (Waters Corp.) was added to the mix to a final concentration of 0.1% and samples were boiled for 5 min. TCEP (Tris (2-carboxyethyl) phosphine) was added to 1 mM (final concentration) and the samples were incubated at 37°C for 30 min. Subsequently, the samples were carboxymethylated with 0.5 mg/ml of iodoacetamide for 30 min at 37°C followed by neutralization with 2 mM TCEP (final concentration). Proteins samples prepared as above were digested with trypsin (trypsin:protein ratio - 1:50) overnight at 37°C. RapiGest was degraded and removed by treating the samples with 250 mM HCl at 37°C for 1 h followed by centrifugation at 14000

rpm for 30 min at 4°C. The soluble fraction was then added to a new tube and the peptides were extracted and desalted using C18 desalting columns (Thermo Scientific).

Trypsin-digested peptides were analyzed by ultra high pressure liquid chromatography (UPLC) coupled with tandem mass spectroscopy (LC-MS/MS) using nano-spray ionization as described[122]. The nano-spray ionization experiments were performed using a TripleTof 5600 hybrid mass spectrometer (ABSCIEX) interfaced with nano-scale reversed-phase UPLC (Waters corporation nano ACQUITY) using a 20 cm-75 micron ID glass capillary packed with 2.5-µm C18 (130) CSH™ beads (Waters corporation). Peptides were eluted from the C18 column into the mass spectrometer using a linear gradient (5–80%) of ACN (acetonitrile) at a flow rate of 250 µl/min for 1 hr. The buffers used to create the ACN gradient were: Buffer A (98% H_2O, 2% ACN, 0.1% formic acid, and 0.005% TFA) and Buffer B (100% ACN, 0.1% formic acid, and 0.005% TFA). MS/MS data were acquired in a data-dependent manner in which the MS1 data was acquired for 250 ms at m/z of 400 to 1250 Da and the MS/MS data was acquired from m/z of 50 to 2,000 Da. The Independent data acquisition (IDA) parameters were as follow; MS1-TOF acquisition time of 250 ms, followed by 50 MS2 events of 48 ms acquisition time for each event. The threshold to trigger MS2 event was set to 150 counts when the ion had the charge state +2, +3 and +4. The ion exclusion time was set to 4 seconds. Finally, the collected data were analyzed using Protein Pilot 4.5 (ABSCIEX) for peptide identifications.

Primers used in this study

Cloning Primers

WT SF-H2A Retro

Forward: TAGATTGAATTCATGTCTGGACGTGGAAAGCAAGG

Reverse: GATATTTGTCGACTCACTTGCCCTTGGCCTTATGGTG

SF- WT H2AX Retro

Forward: TAGATTGGATCCATGTCGGGCCGCGGCAAGACT

Reverse: GATATTTGAATTCGTACTCCTGGGAGGCCTGGGTG

GST CKA1

Forward: ACTGACTGGATCCATGTCGGGACCCGTGCCAAGC

Reverse: ACTGACTGCGGCCGCTTACTGCTGAGCGCCAGCGGC

Mutagenesis Primers

H2A K118R

Forward: GTATTGCTGCCTAGGAAGACGGAGAGCCACC

Reverse: GGTGGCTCTCCGTCTTCCTAGGCAGCAATAC

H2A K118R K119R

Forward: GTATTGCTGCCTAGGCGTACGGAGAGCCACC

Reverse: GGTGGCTCTCCGTACGCCTAGGCAGCAATAC

H2A Y57F

Forward: GCGGTGCTGGAATTTCTGACGGCCGAG

Reverse: CTCGGCCGTCAGAAATTCCAGCACCGC

H2AX S1A

Forward: GACGATAAGGAATTCATGGCGGGCCGCGGCAAG

Reverse: CTTGCCGCGGCCCGCCATGAATTCCTTATCGTC

H2AX T120A

Forward: CTGCTGCCCAAGAAGGCCAGCGCCACCGTG

Reverse: CACGGTGGCGCTGGCCTTCTTGGGCAGCAG

H2AX S121A

Forward: CCCAAGAAGACCGCCGCCACCGTGGG

Reverse: CCCACGGTGGCGGCGGTCTTCTTGGG

H2AX T123A

Forward: CAAGAAGACCAGCGCCGCCGTGGGGCCGAAG

Reverse: CTTCGGCCCCACGGCGGCGCTGGTCTTCTTG

H2AX S130A

Forward: CCGAAGGCGCCCGCGGGCGGCAAGAAG

Reverse: CTTCTTGCCGCCCGCGGGCGCCTTCGG

H2AX T6A

Forward: GGCCGCGGCAAGGCTGGCGGCAAG

Reverse: CTTGCCGCCAGCCTTGCCGCGGCC

H2AX S16A

Forward: GCCAAGGCCAAGGCGCGCTCGTCGC

Reverse: GCGACGAGCGCGCCTTGGCCTTGGC

H2AX S18A

Forward: GCCAAGTCGCGCGCGTCGCGCGCCG

Reverse: CGGCGCGCGACGCGCGCGACTTGGC

H2AX S19A

Forward: CAAGTCGCGCTCGGCGCGCGCCGGCC

Reverse: GGCCGGCGCGCGCCGAGCGCGACTTG

H2AX T59A

Forward: GCTGGAGTACCTCGCCGCTGAGATCCTG

Reverse: CAGGATCTCAGCGGCGAGGTACTCCAGC

H2AX T76A

Forward: CGCGACAACAAGAAGGCGCGAATCATCCCCC

Reverse: GGGGGATGATTCGCGCCTTCTTGTTGTCGCG

H2AX T101A

Forward: CTGGGCGGCGTGGCGATCGCCCAGG

Reverse: CCTGGGCGATCGCCACGCCGCCCAG

H2AX T136A

Forward: GGCAAGAAGGCCGCCCAGGCCTCCC

Reverse: GGGAGGCCTGGGCGGCCTTCTTGCC

H2AX S139A

Forward: GCCACCCAGGCCGCCCAGGAGTACT

Reverse: AGTACTCCTGGGCGGCCTGGGTGGC

H2AX Y39F

Forward: GGAAGGGCCACTTCGCCGAGCGCGTTG

Reverse: CAACGCGCTCGGCGAAGTGGCCCTTCC

H2AX Y50F

Forward: GCGCGCCAGTGTTCCTGGCGGCAGTG

Reverse: CACTGCCGCCAGGAACACTGGCGCGC

H2AX Y57F

Forward: GCAGTGCTGGAGTTCCTCACCGCTGAG

Reverse: CTCAGCGGTGAGGAACTCCAGCACTGC

yH2AZ Y65F

Forward: GACTGCTGTGTTGGAATTTTTGACTGCTGAAGTGC

Reverse: GCACTTCAGCAGTCAAAAATTCCAACACAGCAGTC

yH2A Y58A

Forward: CTTGACTGCTGTCTTGGAAGCTTTGGCCGCTGAAATTTTAG

Reverse: CTAAAATTTCAGCGGCCAAAGCTTCCAAGACAGCAGTCAAG

yH2A Y58F

Forward: CTTGACTGCTGTCTTGGAATTTTGGCCGCTGAAATTTTAG

Reverse: CTAAAATTTCAGCGGCCAAAAATTCCAAGACAGCAGTCAAG

hH2A-Y57F

Forward: GCGGTGCTGGAATTTCTGACGGCCGAG

Reverse: CTCGGCCGTCAGAAATTCCAGCACCGC

hH2A-Y50F

Forward: GGCGCTCCAGTGTTCCTGGCAGCGGTG

Reverse: CACCGCTGCCAGGAACACTGGAGCGCC

hH2A-Y39F

Forward: CTCCGCAAAGGCAACTTCTCCGAACGAGTCGGG

Reverse: CCCGACTCGTTCGGAGAAGTTGCCTTTGCGGAG

qPCR Primers

SSA4

Forward: TTGTGGTACGCCTCTTGGAG

Reverse: CCTACGCTGACAACCAACCT

HSP12

Forward: TCTTCCAAGGTGTCCACGAC

Reverse: CCGGAAACATATTCGACGGC

PYK1

Forward 1: CATATGATGCTAGGTACCTTTAGTGTCTTC

Reverse 1: CAATCTTTCTAATCTAGACATTGTGATGATG

Forward 2: GGTAAGATCTGTTCCCACAAGGGTG

Reverse 2: CAAGTCACCTCTGGCAACCATAACAC

HSP104

Forward: ATGCCGACTCCACCACTAAA

Reverse: CTACGTTCAGCATCAAGGGC

KLK3

Forward: CAGAACTTTCTCCCCATTGC

Reverse: TGAGCCCCACAAAGAGAAAC

KLK2

Forward: TCAGCTGTGAGCATTCAACC

Reverse: TCTGGTGGAATCTGGGTTTC

FKBP5

Forward: ACAGTGTGTTCAGCGTTTGG

Reverse: GGCAAAGAAAGCTCCCATTC

NKX3.1

Forward: AACGCCTCGTTTAGCGAAGA

Reverse: TGCCGTGGAACAAGATACCC

PMA1

Forward 1: ACGATGACGCTGCATCTGAA

Reverse 1: CGTCGTCGACACCGTGATTA

Forward 2: ACCGGTGACAACACTTTCGT

Reverse 2: ACAAGCAGTCCAGACCAACA

YEF3

Forward: TCTTGGGTAAATTGTTGCCAGG

Reverse: GTGCAAGAAGATAGTCATGTATGGGGTG

SCR1

Forward: CGCGGCTAGACACGGAT

Reverse: GCACGGTGCGGAATAGAGAA

Yeast strains used in the study.

Strains (alias) Genotype

LPY5: W303 *MATa*

LPY8241: *MATα ubp8Δ::kanMX*

LPY11654: *MATa htz1Δ::kanMX*

LPY14461: *MATα hht1-hhf1Δ::kanMX hta1-htb1Δ::NatMX hta2-htb2Δ::HPH*+ pJH33

LPY14828: LPY14461+ pLP2133 (no pJH33)

LPY15980: *MATα hht1-hhf1Δ::kanMX hta1-htb1Δ::NatMX hta2-htb2Δ::HPH RTF1-HA::kanMX*+pLP2492

LPY15981: *MATα hht1-hhf1Δ::kanMX hta1-htb1Δ::NatMX hta2-htb2Δ::HPH RTF1-HA::kanMX*+pLP3202

LPY16021: *MATa hht1-hhf1Δ::kanMX hta1-htb1Δ::NatMX hta2-htb2Δ::HPH RAD6-HA::kanMX*+pLP2492

LPY16024: *MATa hht1-hhf1Δ::kanMX hta1-htb1Δ::NatMX hta2-htb2Δ::HPH RAD6-HA::kanMX*+pLP3202

LPY16265* (KY2248): *MATα his3Δ200 lys2-128δ leu2Δ1 trp1Δ63 ura3-52 hta1-htb1Δ::LEU2 hta2-htb2Δ::kanMX ubp8Δ::NatMX*+pDC92

LPY16266* (KY1600): *MATα his3Δ200 lys2-128δ leu2Δ1 trp1Δ63 ura3-52 hta1-htb1Δ::LEU2 hta2-htb2Δ::kanMX*+pSAB6

LPY16267*: LPY16266+pLP2492 (no pSAB6)

LPY16269*: LPY16266+pLP3202 (no pSAB6)

LPY16563*: LPY16265+pLP2492 (no pDC92)

LPY16565*: LPY16265+pLP3202 (no pDC92)

LPY17876: LPY14461+ pLP2492 (no pJH33)

LPY17878: LPY14461+ pLP3202 (no pJH33)

LPY18606: LPY14461+ pLP2908 (no pJH33)

LPY18192: *MATα hht1-hhf1Δ::URA3 hta1-htb1Δ::NatMX hta2-htb2Δ::HPH*+ pLP2492

LPY18194: *MATα hht1-hhf1Δ::URA3 hta1-htb1Δ::NatMX hta2-htb2Δ::HPH*+ pLP3202

LPY19236: *MATa hht1-hhf1Δ::kanMX hta1-htb1Δ::NatMX hta2-htb2Δ::HPH htz1Δ::kanMX* +pJH33

LPY19259: LPY19236+pLP2492

LPY19261: LPY19236+pLP3202

LPY19265: *MATα hht1-hhf1Δ::kanMX hta1-htb1Δ::NatMX hta2-htb2Δ::HPH PAF1-MYC::kanMX*+pLP2492

LPY19266: *MATα hht1-hhf1Δ::kanMX hta1-htb1Δ::NatMX hta2-htb2Δ::HPH PAF1-MYC::kanMX*+pLP3202

LPY19464: LPY14461+pLP3213 (no pJH33)

LPY19806: LPY19236+pLP2252+pLP3202 (no pJH33)

LPY19894: LPY19236+pLP3200+pLP3202 (no pJH33)

Except where indicated by *, all strains are in the W303 background. Unless otherwise stated, the strains were constructed during this study or are part of the Pillus lab collection.

Yeast plasmids used in the study.

Plasmid (alias)	Description
pJH33	*HTA1-HTB1 HHF2-HHT2 URA3* CEN
pRS313	vector *HIS3* CEN
pRS314	vector *TRP1* CEN
pLP2133	pRS313-Flag-*HTA1-HTB1*
pLP2492	pRS313-*HTA1* Flag-*HTB1*
pLP2252	pRS314-*HTZ1*
pLP2908	pRS313-*HTA1*-Flag-*htb1-K123R*
pLP3200	pRS314-*htz1-Y65F*
pLP3202	pRS313-*hta1-Y58F*-Flag-*HTB1*
pLP3211	pRS313-Flag-*hta1-Y58A-HTB1*

pLP3213 pRS313-Flag-*hta1-Y58F-HTB1*

Appendix, in most part, is a reprint of the material that has been accepted for publication as it may appear in *Nature* 2014. Basnet, Harihar; Su, Xue B.; Tan, Yuliang; Meisenhelder, Jill; Merkurjev, Daria; Ohgi, Kenneth A.; Hunter, Tony; Pillus, Lorraine & Rosenfeld Michael G. Nature Publishing Group. 2014. The dissertation author was the primary investigator and author of this paper.

References

1. Luger, K., Mäder, A. W., Richmond, R. K., Sargent, D. F. & Richmond, T. J. Crystal structure of the nucleosome core particle at 2.8 A resolution. *Nature* **389,** 251–260 (1997).

2. Orsi, G. A., Couble, P. & Loppin, B. Epigenetic and replacement roles of histone variant H3.3 in reproduction and development. *Int. J. Dev. Biol.* **53,** 231–243 (2009).

3. Kamakaka, R. T. & Biggins, S. Histone variants: deviants? *Genes Dev.* **19,** 295–316 (2005).

4. Banaszynski, L. A., Allis, C. D. & Lewis, P. W. Histone variants in metazoan development. *Dev. Cell* **19,** 662–674 (2010).

5. Sarma, K. & Reinberg, D. Histone variants meet their match. *Nat. Rev. Mol. Cell Biol.* **6,** 139–149 (2005).

6. Wu, T., Yuan, T., Wang, C., Sun, S., Lam, H. & Ngai, S. Mass spectrometry analysis of the variants of histone H3 and H4 of soybean and their post-translational modifications. *BMC Plant Biol.* **9,** 98 (2009).

7. Elsaesser, S. J., Goldberg, A. D. & Allis, C. D. New functions for an old variant: no substitute for histone H3.3. *Curr. Opin. Genet. Dev.* **20,** 110–117 (2010).

8. Shi, L., Wang, J., Hong, F., Spector, D. L. & Fang, Y. Four amino acids guide the assembly or disassembly of Arabidopsis histone H3.3-containing nucleosomes. *Proc. Natl. Acad. Sci. U. S. A.* **108,** 10574–10578 (2011).

9. Rogakou, E. P., Nieves-Neira, W., Boon, C., Pommier, Y. & Bonner, W. M. Initiation of DNA Fragmentation during Apoptosis Induces Phosphorylation of H2AX Histone at Serine 139. *J. Biol. Chem.* **275,** 9390–9395 (2000).

10. Cook, P. J., Ju, B. G., Telese, F., Wang, X., Glass, C. K. & Rosenfeld, M. G. Tyrosine dephosphorylation of H2AX modulates apoptosis and survival decisions. *Nature* **458,** 591–596 (2009).

11. Xiao, A., Li, H., Schecter, D., Ahn, S. H., Fabrizio, L. A., Erdjument-Bromage, H., Ishibe-Murakami, S., Wang, B., Tempst, P., Hafman, K., Patel, D. J., Elledge, S. J. & Allis, C. D. WSTF regulates the H2A.X DNA damage response via a novel tyrosine kinase activity. *Nature* **457,** 57–62 (2009).

12. Kouzarides, T. Chromatin Modifications and Their Function. *Cell* **128,** 693–705 (2007).

13. Strahl, B. D. & Allis, C. D. The language of covalent histone modifications. *Nature* **403,** 41–45 (2000).

14. Jung, H. R., Pasini, D., Helin, K. & Jensen, O. N. Quantitative Mass Spectrometry of Histones H3.2 and H3.3 in Suz12-deficient Mouse Embryonic Stem Cells Reveals Distinct, Dynamic Post-translational Modifications at Lys-27 and Lys-36. *Mol. Cell. Proteomics* **9,** 838–850 (2010).

15. Wang, Y., Reddy, B., Thompson, J., Wang, H., Noma, K., Yates, J. R. & Jia, S. Regulation of Set9-mediated H4K20 methylation by a PWWP domain protein. *Mol. Cell* **33,** 428–437 (2009).

16. Marmorstein, R. & Berger, S. L. Structure and function of bromodomains in chromatin-regulating complexes. *Gene* **272,** 1–9 (2001).

17. Soulier, J. & Lowndes, N. F. The BRCT domain of the S. cerevisiae checkpoint protein Rad9 mediates a Rad9–Rad9 interaction after DNA damage. *Curr. Biol.* **9,** 551–S2 (1999).

18. Lancelot, N., Charier, G., Couprie, J., Duband-Goulet, I., Alpha-Bazin, B., Quemeneur, E., Ma, E., Marsolier-Kergoat, M., Ropars, V., Charbonnier, J., Miron, S., Craescu, C. T., Callebaut, I., Gilquin, B. & Zinn-Justin, S. The checkpoint Saccharomyces cerevisiae Rad9 protein contains a tandem tudor domain that recognizes DNA. *Nucleic Acids Res.* **35,** 5898–5912 (2007).

19. Clapperton, J. A., Manke, I. A., Lowery, D. M., Ho, T., Haire, L. F., Yaffe, M. B. & Smerdon, S. J. Structure and mechanism of BRCA1 BRCT domain recognition of phosphorylated BACH1 with implications for cancer. *Nat. Struct. Mol. Biol.* **11,** 512–518 (2004).

20. Singh, N., Basnet, H., Wiltshire, T. D., Mohammad, D. H., Thompson, J. R., Heroux, A., Botuyan, M. V., Yaffe, M. B., Couch, F. J., Rosenfeld, M. G. & Mer, G. Dual recognition of phosphoserine and phosphotyrosine in histone variant H2A.X by DNA damage response protein MCPH1. *Proc. Natl. Acad. Sci.* **109,** 14381–14386 (2012).

21. Sun, Z., Hsiao, J., Fay, D. S. & Stern, D. F. Rad53 FHA Domain Associated with Phosphorylated Rad9 in the DNA Damage Checkpoint. *Science* **281,** 272–274 (1998).

22. Shi, X., Hong, T., Walter, K. L., Ewalt, M., Michishita, E., Hung, T., Carney, D., Pena, P., Lan, F., Kaadige, M. R., Lacoste, N., Cayrou, C., Davrazou, F., Saha, A., Cairns, B. R., Ayer, D. E., Kutateladze, T. G., Shi, Y., Cote, J., Chua, K. F. & Gozani, O. ING2 PHD domain links histone H3 lysine 4 methylation to active gene repression. *Nature* **442,** 96–99 (2006).

23. Moran, M. F., Koch, C. A., Anderson, D., Ellis, C., England, L., Martin, G. S. & Pawson, T. Src homology region 2 domains direct protein-protein interactions in signal transduction. *Proc. Natl. Acad. Sci. U. S. A.* **87,** 8622–8626 (1990).

24. Hwang, W. L., Deindl, S., Harada, B. T. & Zhuang, X. Histone H4 tail mediates allosteric regulation of nucleosome remodelling by linker DNA. *Nature* **advance online publication,** (2014).

25. Schmitges, F. W., Prusty, A. B., Faty, M., Stutzer, A., Lingaraju, G., Aiwazian, J., Sack, R., Hess, D., Li, L., Zhou, S., Bunker, R. D., Wirth, U., Bouwmeester, T., Bauer, A., Ly-Hartig, N., Zhao, K., Chan, H., Gu, J. Gut, H., Fischle, W., Muller, J. & Thoma, N. H. Histone Methylation by PRC2 Is Inhibited by Active Chromatin Marks. *Mol. Cell* **42,** 330–341 (2011).

26. Li, B., Huang, Z., Cui, Q., Song, X., Du, L., Jeltsch, A., Chen, P., Li, G., Li, E. & Xu, G. Histone tails regulate DNA methylation by allosterically activating de novo methyltransferase. *Cell Res.* **21,** 1172–1181 (2011).

27. Phanstiel, D., Brumbaugh, J., Berggren, W. T., Conard, K., Feng, X., Levenstein, M. E., Thonson, J. A. & Coon, J. J. Mass spectrometry identifies and quantifies 74 unique histone H4 isoforms in differentiating human embryonic stem cells. *Proc. Natl. Acad. Sci.* **105,** 4093–4098 (2008).

28. Jason, L. J. M., Moore, S. C., Lewis, J. D., Lindsey, G. & Ausió, J. Histone ubiquitination: a tagging tail unfolds? *BioEssays News Rev. Mol. Cell. Dev. Biol.* **24,** 166–174 (2002).

29. Scheffner, M., Nuber, U. & Huibregtse, J. M. Protein ubiquitination involving an E1-E2-E3 enzyme ubiquitin thioester cascade. *Nature* **373,** 81–83 (1995).

30. Glickman, M. H. & Ciechanover, A. The ubiquitin-proteasome proteolytic pathway: destruction for the sake of construction. *Physiol. Rev.* **82,** 373–428 (2002).

31. Spence, J., Gali, R. R., Dittmar, G., Sherman, F., Karin, M. & Finley, D. Cell cycle-regulated modification of the ribosome by a variant multiubiquitin chain. *Cell* **102,** 67–76 (2000).

32. Wilkinson, K. D. Regulation of ubiquitin-dependent processes by deubiquitinating enzymes. *FASEB J. Off. Publ. Fed. Am. Soc. Exp. Biol.* **11,** 1245–1256 (1997).

33. West, M. H. & Bonner, W. M. Histone 2B can be modified by the attachment of ubiquitin. *Nucleic Acids Res.* **8,** 4671–4680 (1980).

34. Wang, H., Zhai, L., Xu, J., Joo, H., Jackson, S., Erdjument-Bromage, H., Tempst, P., Xiong, Y. & Zhang, Y. Histone H3 and H4 ubiquitylation by the CUL4-DDB-ROC1 ubiquitin ligase facilitates cellular response to DNA damage. *Mol. Cell* **22,** 383–394 (2006).

35. Goldknopf, I. L., Taylor, C. W., Baum, R. M., Yeoman, L. C., Olson, M. O., Prestayko, A. W. & Busch, H. Isolation and characterization of protein A24, a ‘histone-like’ non-histone chromosomal protein. *J. Biol. Chem.* **250,** 7182–7187 (1975).

36. Pham, A. D. & Sauer, F. Ubiquitin-activating/conjugating activity of TAFII250, a mediator of activation of gene expression in Drosophila. *Science* **289,** 2357–2360 (2000).

37. Cao, J. & Yan, Q. Histone Ubiquitination and Deubiquitination in Transcription, DNA Damage Response, and Cancer. *Front. Oncol.* **2,** (2012).

38. Scheuermann, J. C., de Ayala Alonso, A., Oktaba, K., Ly-Hartig, N., McGinty, R. K., Fraterman, S., Wilm, M., Muir, T. W. & Muller, J. Histone H2A deubiquitinase activity of the Polycomb repressive complex PR-DUB. *Nature* **465,** 243–247 (2010).

39. Zhou, W., Zhu, P., Wang, J., Pascual, G., Ohgi, K. A., Lozach, J., Glass, C. K. & Rosenfeld, M. G. Histone H2A Monoubiquitination Represses Transcription by Inhibiting RNA Polymerase II Transcriptional Elongation. *Mol. Cell* **29,** 69–80 (2008).

40. Zhu, P., Zhou, W., Wang, J., Puc, J., Ohgi, K. A., Erdjument-Bromage, H., Tempst, P., Glass, C. K. & Rosenfeld, M. G. A histone H2A deubiquitinase complex coordinating histone acetylation and H1 dissociation in transcriptional regulation. *Mol. Cell* **27,** 609–621 (2007).

41. Gatti, M., Pinato, S., Maspero, E., Soffientini, P., Polo, S. & Penengo, L. A novel ubiquitin mark at the N-terminal tail of histone H2As targeted by RNF168 ubiquitin ligase. *Cell Cycle Georget. Tex* **11,** 2538–2544 (2012).

42. Ismail, I. H., Andrin, C., McDonald, D. & Hendzel, M. J. BMI1-mediated histone ubiquitylation promotes DNA double-strand break repair. *J. Cell Biol.* **191,** 45–60 (2010).

43. Nakagawa, T., Kajitani, T., Togo, S., Masuko, N., Ohdan, H., Hishikawa, Y., Koji, T., Matsuyama, T., Ikura, T., Muramatsu, M. & Ito, T. Deubiquitylation of histone H2A activates transcriptional initiation via trans-histone cross-talk with H3K4 di- and trimethylation. *Genes Dev.* **22,** 37–49 (2008).

44. Lee, J.-S., Shukla, A., Schneider, J., Swanson, S. K., Washburn, M. P., Florens, L., Bhaumik, S. R. & Shilatifard, A. Histone crosstalk between H2B

monoubiquitination and H3 methylation mediated by COMPASS. *Cell* **131,** 1084–1096 (2007).

45. Xiao, T., Kao, C-F., Krogan, N. J., Sun, Z-W., Greenblat, J. F., Osley, M. A. & Strahl, B. D. Histone H2B ubiquitylation is associated with elongating RNA polymerase II. *Mol. Cell. Biol.* **25,** 637–651 (2005).

46. De Napoles, M., Mermoud, J. E., Wakao, R., Tang, Y. A., Endoh, M., Appanah, R., Nesterova, T. B., Silva, J., Otte, A. P., Vidal, M., Koseki, H. & Brockdroff, N. Polycomb group proteins Ring1A/B link ubiquitylation of histone H2A to heritable gene silencing and X inactivation. *Dev. Cell* **7,** 663–676 (2004).

47. Mattiroli, F., Vissers, J. H., Van Dijk, W. J., Ikpa, P., Citterio, E., Vermeulen, W., Marteijn, J. A., & Sixma, T. K. RNF168 ubiquitinates K13-15 on H2A/H2AX to drive DNA damage signaling. *Cell* **150,** 1182–1195 (2012).

48. Tanny, J. C., Erdjument-Bromage, H., Tempst, P. & Allis, C. D. Ubiquitylation of histone H2B controls RNA polymerase II transcription elongation independently of histone H3 methylation. *Genes Dev.* **21,** 835–847 (2007).

49. Weake, V. M. & Workman, J. L. Histone ubiquitination: triggering gene activity. *Mol. Cell* **29,** 653–663 (2008).

50. Robzyk, K., Recht, J. & Osley, M. A. Rad6-Dependent Ubiquitination of Histone H2B in Yeast. *Science* **287,** 501–504 (2000).

51. Wood, A., Schneider, J., Dover, J., Johnston, M. & Shilatifard, A. The Paf1 complex is essential for histone monoubiquitination by the Rad6-Bre1 complex, which signals for histone methylation by COMPASS and Dot1p. *J. Biol. Chem.* **278,** 34739–34742 (2003).

52. Sun, Z.-W. & Allis, C. D. Ubiquitination of histone H2B regulates H3 methylation and gene silencing in yeast. *Nature* **418,** 104–108 (2002).

53. Mueller, C. L. & Jaehning, J. A. Ctr9, Rtf1, and Leo1 Are Components of the Paf1/RNA Polymerase II Complex. *Mol. Cell. Biol.* **22,** 1971–1980 (2002).

54. Ng, H. H., Dole, S. & Struhl, K. The Rtf1 Component of the Paf1 Transcriptional Elongation Complex Is Required for Ubiquitination of Histone H2B. *J. Biol. Chem.* **278,** 33625–33628 (2003).

55. Henry, K. W., Wyce, A., Lo, W-S., Duggan, L. J., Emre, N. C. T., Pillus, L., Shilatifard, A. & Berger, S. L. Transcriptional activation via sequential histone H2B ubiquitylation and deubiquitylation, mediated by SAGA-associated Ubp8. *Genes Dev.* **17,** 2648–2663 (2003).

56. Gardner, R. G., Nelson, Z. W. & Gottschling, D. E. Ubp10/Dot4p regulates the persistence of ubiquitinated histone H2B: distinct roles in telomeric silencing and general chromatin. *Mol. Cell. Biol.* **25,** 6123–6139 (2005).

57. Emre, N. C. T., Ingvarsdottir, K., Wyce, A., Wood, A., Krogan, N. J., Henry, K. W., Li, K., Marmorstein, R., Greenblatt, J. F., Shilatifard, A. & BErger, S. L. Maintenance of low histone ubiquitylation by Ubp10 correlates with telomere-proximal Sir2 association and gene silencing. *Mol. Cell* **17,** 585–594 (2005).

58. Zhang, Y. Transcriptional regulation by histone ubiquitination and deubiquitination. *Genes Dev.* **17,** 2733–2740 (2003).

59. Lilley, C. E., Chaurushiya, M. S., Boutell, C., Landry, S., Suh, J., Panier, S., Everett, R. D., Stewart, G. S., Durocher, D. & Weitzman, M. D. A viral E3 ligase targets RNF8 and RNF168 to control histone ubiquitination and DNA damage responses. *EMBO J.* **29,** 943–955 (2010).

60. Thakar, A., Parvin, J. D. & Zlatanova, J. BRCA1/BARD1 E3 Ubiquitin Ligase Can Modify Histones H2A and H2B in the Nucleosome Particle. *J. Biomol. Struct. Dyn.* **27,** 399–405 (2010).

61. Huen, M. S. Y., Grant, R., Manke, I., Minn, K., Yu, X., Yaffe, M. B. & Chen, J. The E3 ubiquitin ligase RNF8 transduces the DNA damage signal via an ubiquitin-dependent signaling pathway. *Cell* **131,** 901–914 (2007).

62. Wang, H., Wang, L., Erdjument-Bromage, H., Vidal, M., Tempst, P., Jones, R. S. & Zhang, Y. Role of histone H2A ubiquitination in Polycomb silencing. *Nature* **431,** 873–878 (2004).

63. Joo, H.-Y., Zhai, L., Yang, C., Nie, S., Erdjument-Bromage, H., Tempst, P., Chang, C. & Wang, H. Regulation of cell cycle progression and gene expression by H2A deubiquitination. *Nature* **449,** 1068–1072 (2007).

64. Lang, G., Bonnet, J., Umlauf, D., Karmodiya, K., Koffler, J., Stierle, M., Devys, D. & Tora, L. The Tightly Controlled Deubiquitination Activity of the Human SAGA Complex Differentially Modifies Distinct Gene Regulatory Elements. *Mol. Cell. Biol.* **31,** 3734–3744 (2011).

65. Schoeftner, S., Sengupta, A. K., Kubicek, S., Mechtler, K., Spahn, L., Koseki, H., Jenuwein, T. & Wutz, A. Recruitment of PRC1 function at the initiation of X inactivation independent of PRC2 and silencing. *EMBO J.* **25,** 3110–3122 (2006).

66. Schaaf, C. A., Misulovin, Z., Gause, M., Koenig, A., Gohara, D. W., Watson, A. & Dorsett, D. Cohesin and polycomb proteins functionally interact to control transcription at silenced and active genes. *PLoS Genet.* **9,** e1003560 (2013).

67. Cao, R., Wang, L., Wang, H., Xia, L., Erdjument-Bromage, H., Tempst, P., Jones, R. S. & Zhang, Y. Role of histone H3 lysine 27 methylation in Polycomb-group silencing. *Science* **298,** 1039–1043 (2002).

68. Pasini, D., Bracken, A. P., Hansen, J. B., Capillo, M. & Helin, K. The polycomb group protein Suz12 is required for embryonic stem cell differentiation. *Mol. Cell. Biol.* **27,** 3769–3779 (2007).

69. Min, J., Zhang, Y. & Xu, R.-M. Structural basis for specific binding of Polycomb chromodomain to histone H3 methylated at Lys 27. *Genes Dev.* **17,** 1823–1828 (2003).

70. Boyer, L. A., Plath, K., Zeitlinger, J., Brambrink, T., Medeiros, L. A., Lee, T. I., Levine, S. S., Tajonar, A., Ray, M. K., Bell, G. W., Otte, A. P., Vidal, M., Gifford, D. K., Young, R. A. & Jaenisch, R. Polycomb complexes repress

developmental regulators in murine embryonic stem cells. *Nature* **441,** 349–353 (2006).

71. Leeb, M., Pasini, D., Novatchkova, M., Jaritz, M., Helin, K. & Wutz, A. Polycomb complexes act redundantly to repress genomic repeats and genes. *Genes Dev.* **24,** 265–276 (2010).

72. Ku, M., Koche, R. P., Rheinbay, E., Mendenhall, E. M., Endoh, M., Mikkelsen, T. S., Presser, A., Nausbam, C., Xie, X., Chi, A. S., Adli, M., Kasif, S., Ptaszek, L. M., Cowan, C. A., Lander, E. S., Koseki, H. & Bernstein, B. E. Genomewide analysis of PRC1 and PRC2 occupancy identifies two classes of bivalent domains. *PLoS Genet.* **4,** e1000242 (2008).

73. Suganuma, T. & Workman, J. L. Crosstalk among Histone Modifications. *Cell* **135,** 604–607 (2008).

74. Segre, C. V. & Chiocca, S. Regulating the Regulators: The Post-Translational Code of Class I HDAC1 and HDAC2. *BioMed Res. Int.* **2011,** e690848 (2010).

75. Li, Y., Kao, G. D., Garcia, B. A., Shabanowitz, J., Hunt, D. F., Qin, J., Phelan, C. & Lazar, M. A. A novel histone deacetylase pathway regulates mitosis by modulating Aurora B kinase activity. *Genes Dev.* **20,** 2566–2579 (2006).

76. Hunter, T. The age of crosstalk: phosphorylation, ubiquitination, and beyond. *Mol. Cell* **28,** 730–738 (2007).

77. Stucki, M., Clapperton, J. A., Mohammad, D., Yaffe, M. B. Semrdon, S. J. & Jackson, S. P. MDC1 directly binds phosphorylated histone H2AX to regulate cellular responses to DNA double-strand breaks. *Cell* **123,** 1213–1226 (2005).

78. Rappold, I., Iwabuchi, K., Date, T. & Chen, J. Tumor Suppressor P53 Binding Protein 1 (53bp1) Is Involved in DNA Damage–Signaling Pathways. *J. Cell Biol.* **153,** 613–620 (2001).

79. Nakanishi, S., Sanderson, B. W., Delventhal, K. M., Bradford, W. D., Staehling-Hampton, K. & Shilatifard, A. A comprehensive library of histone mutants identifies nucleosomal residues required for H3K4 methylation. *Nat. Struct. Mol. Biol.* **15,** 881–888 (2008).

80. Dai, J., Hyland, E. M., Yuan, D. S., Huang, H., Bader, J. S. & Boeke, J. D. Probing nucleosome function: a highly versatile library of synthetic histone H3 and H4 mutants. *Cell* **134,** 1066–1078 (2008).

81. Latham, J. A. & Dent, S. Y. R. Cross-regulation of histone modifications. *Nat. Struct. Mol. Biol.* **14,** 1017–1024 (2007).

82. Mahajan, K., Fang, B., Koomen, J. M. & Mahajan, N. P. H2B Tyr37 phosphorylation suppresses expression of replication-dependent core histone genes. *Nat. Struct. Mol. Biol.* **19,** 930–937 (2012).

83. Mizuguchi, G., Shen, X., Wu, W-H., Sen, S. & Wu, C. ATP-Driven Exchange of Histone H2AZ Variant Catalyzed by SWR1 Chromatin Remodeling Complex. *Science* **303,** 343–348 (2004).

84. Kobor, M. S., Venkatasubrahmanyam, S., Gin, J. W., Jennings, J. L., Link, A. J., Madhani, H. D. & Rine, J. A protein complex containing the conserved Swi2/Snf2-related ATPase Swr1p deposits histone variant H2A.Z into euchromatin. *PLoS Biol.* **2,** E131 (2004).

85. Krogan, N. J., Keogh, M-C., Datta, N., Sawa, C., Ryan, O. W., Ding, H., Haw, R. A., Pootoolal, J., Tong, A., Canadien, V., Richards, D. P., Wu, X., Emili, A., Hughes, T. R., Buratowski, S. & Greenblatt, J. F. A Snf2 family ATPase complex required for recruitment of the histone H2A variant Htz1. *Mol. Cell* **12,** 1565–1576 (2003).

86. Adam, M., Robert, F., Larochelle, M. & Gaudreau, L. H2A.Z is required for global chromatin integrity and for recruitment of RNA polymerase II under specific conditions. *Mol. Cell. Biol.* **21,** 6270–6279 (2001).

87. Stucki, M. & Jackson, S. P. gammaH2AX and MDC1: anchoring the DNA-damage-response machinery to broken chromosomes. *DNA Repair* **5,** 534–543 (2006).

88. Bekker-Jensen, S., Lukas, C., Kitagawa, R., Melander, F., Kastan, M. B., Bartek, J. & Lukas, J. Spatial organization of the mammalian genome surveillance machinery in response to DNA strand breaks. *J. Cell Biol.* **173,** 195–206 (2006).

89. Kizer, K. O., Phatnani, H. P., Shibata, Y., Hall, H., Greenleaf, A. L. & Strahl, B. D. A novel domain in Set2 mediates RNA polymerase II interaction and couples histone H3 K36 methylation with transcript elongation. *Mol. Cell. Biol.* **25,** 3305–3316 (2005).

90. Kouskouti, A. & Talianidis, I. Histone modifications defining active genes persist after transcriptional and mitotic inactivation. *EMBO J.* **24,** 347–357 (2005).

91. Krogan, N. J., Dover, J., Wood, A., Schneider, J., Heidt, J., Boateng, M. A., Dean, K., Ryan, O. W., Golshani, A., Johnston, M., Greenblatt, J. F. & Shilatifard, A. The Paf1 complex is required for histone H3 methylation by COMPASS and Dot1p: linking transcriptional elongation to histone methylation. *Mol. Cell* **11,** 721–729 (2003).

92. Wei, Y., Mizzen, C. A., Cook, R. G., Gorovsky, M. A. & Allis, C. D. Phosphorylation of histone H3 at serine 10 is correlated with chromosome condensation during mitosis and meiosis in Tetrahymena. *Proc. Natl. Acad. Sci. U. S. A.* **95,** 7480–7484 (1998).

93. Wei, Y., Yu, L., Bowen, J., Gorovsky, M. A. & Allis, C. D. Phosphorylation of Histone H3 Is Required for Proper Chromosome Condensation and Segregation. *Cell* **97,** 99–109 (1999).

94. Ferguson, S. B., Anderson, E. S., Harshaw, R. B., Thate, T., Craig, N. L. & Nelson, H. C. M. Protein kinase A regulates constitutive expression of small heat-shock genes in an Msn2/4p-independent and Hsf1p-dependent manner in Saccharomyces cerevisiae. *Genetics* **169,** 1203–1214 (2005).

95. Chao, S.-H. & Price, D. H. Flavopiridol Inactivates P-TEFb and Blocks Most RNA Polymerase II Transcription in Vivo. *J. Biol. Chem.* **276,** 31793–31799 (2001).

96. Kim, J., Guermah, M., McGinty, R. K., Lee, J-S., Tang, Z., Milne, T. A., Shilatifard, A., Muir, T. W. & Roeder, R. G. RAD6-Mediated transcription-coupled H2B ubiquitylation directly stimulates H3K4 methylation in human cells. *Cell* **137,** 459–471 (2009).

97. Thornton, J. L., Westfield, G. H., Takahashi, Y-H., Cook, M., Woodfin, A. R., Lee, J-S., Morgan, M. A., Jackson, J., Smith, E. R., Couture, J-F., Skiniotis, G. & Shilatifard, A. Context dependency of Set1/COMPASS-mediated histone H3 Lys4 trimethylation. *Genes Dev.* **28,** 115–120 (2014).

98. Vilk, G., Weber, J. E., Turowec, J. P., Duncan, J. S., Wu, C., Derksen, D. R., Zien, P., Sarno, S., Donella-Deana, A., Lajoie, G., Pinna, L. A., Li, S. S. C. & Litchfield, D. W. Protein kinase CK2 catalyzes tyrosine phosphorylation in mammalian cells. *Cell. Signal.* **20,** 1942–1951 (2008).

99. Wilson, L. K., Dhillon, N., Thorner, J. & Martin, G. S. Casein kinase II catalyzes tyrosine phosphorylation of the yeast nucleolar immunophilin Fpr3. *J. Biol. Chem.* **272,** 12961–12967 (1997).

100. Liu, W., Tanasa, B., Tyurina, O. V., Zhou, T. Y., Gassmann, R., Liu, W. T., Ohgi, K .A., Benner, C., Garcia-Bassets, I., Aggarwal, A. K., Desai, A., Dorrestein, P. C., Glass, C. K. & Rosenfeld, M. G. PHF8 mediates histone H4 lysine 20 demethylation events involved in cell cycle progression. *Nature* **466,** 508–512 (2010).

101. Pagano, M. A., Meggio, F., Ruzzene, M., Andrzejewska, M., Kazimierczuk, Z. & Pinna, L. A. 2-Dimethylamino-4,5,6,7-tetrabromo-1H-benzimidazole: a novel powerful and selective inhibitor of protein kinase CK2. *Biochem. Biophys. Res. Commun.* **321,** 1040–1044 (2004).

102. Reppas, N. B., Wade, J. T., Church, G. M. & Struhl, K. The transition between transcriptional initiation and elongation in E. coli is highly variable and often rate limiting. *Mol. Cell* **24,** 747–757 (2006).

103. Rahl, P. B., Lin, C. Y., Seila, A. C., Flynn, R. A., McCuine, S., Burge, C. B., Sharp, P. A. & Young, R. A. c-Myc regulates transcriptional pause release. *Cell* **141,** 432–445 (2010).

104. Wang, D., Garcia-Bassets, I., Benner, C., Li, W., Su, X., Zhou, Y., Qui, J., Liu, W., Kaikkonen, M. U., Ohgi, K. A., Glass, C. K., Rosenfeld, M. G. & Fu, X-D. Reprogramming transcription by distinct classes of enhancers functionally defined by eRNA. *Nature* **474,** 390–394 (2011).

105. Meggio, F. & Pinna, L. A. One-thousand-and-one substrates of protein kinase CK2? *FASEB J. Off. Publ. Fed. Am. Soc. Exp. Biol.* **17,** 349–368 (2003).

106. Wade, J. T. & Struhl, K. The transition from transcriptional initiation to elongation. *Curr. Opin. Genet. Dev.* **18,** 130–136 (2008).

107. Shin, H., Liu, T., Manrai, A. K. & Liu, X. S. CEAS: cis-regulatory element annotation system. *Bioinforma. Oxf. Engl.* **25,** 2605–2606 (2009).

108. Heintzman, N. D., Hon, G. C., Hawkins, R. D., Kheradpour, P., Stark, A., Harp, L. F., Ye, Z., Lee, L. K., Stuart, R. K., Ching, C. W., Ching, K. A., Antosiewicz, J. E., Liu, H., Zhang, X., Green, R. D., Stewart, R., Thomson, J. A., Crawford, G. E., Kellis, M. & Ren, B. Histone Modifications at Human Enhancers Reflect Global Cell Type-Specific Gene Expression. *Nature* **459,** 108–112 (2009).

109. Hah, N., Murakami, S., Nagari, A., Danko, C. G. & Kraus, W. L. Enhancer transcripts mark active estrogen receptor binding sites. *Genome Res.* **23,** 1210–1223 (2013).

110. Li, W., Notani, D., Ma, Q., Tanasa, B., Nunez, E., Chen, A. Y., Merkurjev, D., Zhang, J., Ohgi, K. A., Song, X., Oh, S., Kim, H.-S., Glass, C. K. & Rosenfeld, M. G. Functional roles of enhancer RNAs for oestrogen-dependent transcriptional activation. *Nature* **498,** 516–520 (2013).

111. Kim, T.-K., Hemberg, M., Gray, J. M., Costa, A. M., Bear, D. M., Wu, J., Harmin, D. A., Laptewicz, M., Barbara-Haley, K., Kuersten, S., Markenscoff-Papadimitriou, E., Kuhl, D., Bito, H., Worley, P. F., Kreiman, G. & Greenberg, M. E. Widespread transcription at neuronal activity-regulated enhancers. *Nature* **465,** 182–187 (2010).

112. Matsubara, K., Sano, N., Umehara, T. & Horikoshi, M. Global analysis of functional surfaces of core histones with comprehensive point mutants. *Genes Cells Devoted Mol. Cell. Mech.* **12,** 13–33 (2007).

113. Sakamoto, M., Noguchi, S., Kawashima, S., Okada, Y., Enomoto, T., Seki, M. & Horikoshi, M. Global analysis of mutual interaction surfaces of nucleosomes with comprehensive point mutants. *Genes Cells* **14,** 1271–1330 (2009).

114. Sarno, S., Vaglio, P., Marin, O., Issinger, O. G., Ruffato, K. & Pinna, L. A. Mutational analysis of residues implicated in the interaction between protein kinase CK2 and peptide substrates. *Biochemistry (Mosc.)* **36,** 11717–11724 (1997).

115. Krogan, N. J., Kim, M., Ahn, S. H., Zhong, G., Kobor, M. S., Cagney, G., Emili, A., Shilatifard, A., Buratowski, S. & Greenblatt, J. F. RNA Polymerase II Elongation Factors of Saccharomyces cerevisiae: a Targeted Proteomics Approach. *Mol. Cell. Biol.* **22,** 6979–6992 (2002).

116. Suka, N., Suka, Y., Carmen, A. A., Wu, J. & Grunstein, M. Highly Specific Antibodies Determine Histone Acetylation Site Usage in Yeast Heterochromatin and Euchromatin. *Mol. Cell* **8,** 473–479 (2001).

117. Wu, P.-Y. J., Ruhlmann, C., Winston, F. & Schultz, P. Molecular Architecture of the S. cerevisiae SAGA Complex. *Mol. Cell* **15,** 199–208 (2004).

118. O'Neill, L. P. & Turner, B. M. Immunoprecipitation of native chromatin: NChIP. *Methods San Diego Calif* **31,** 76–82 (2003).

119. Strahl-Bolsinger, S., Hecht, A., Luo, K. & Grunstein, M. SIR2 and SIR4 interactions differ in core and extended telomeric heterochromatin in yeast. *Genes Dev.* **11,** 83–93 (1997).

120. Kamps, M. P. & Sefton, B. M. Acid and base hydrolysis of phosphoproteins bound to immobilon facilitates analysis of phosphoamino acids in gel-fractionated proteins. *Anal. Biochem.* **176,** 22–27 (1989).

121. Guttman, M., Betts, G. N., Barnes, H., Ghassemian, M., Van der Geer, P. & Komives, E. A. Interactions of the NPXY microdomains of the low density lipoprotein receptor-related protein 1. *Proteomics* **9,** 5016–5028 (2009).

122. McCormack, A. L., Schieltz, D. M., Goode, B., Yang, S., Barnes, G., Durbin, D. & Yates, J. R. Direct analysis and identification of proteins in mixtures by LC/MS/MS and database searching at the low-femtomole level. *Anal. Chem.* **69,** 767–776 (1997).